# Nutritionally responsive PMv DAT neurons are dynamically regulated during pubertal transition

Cristina Sáenz de Miera[a], Nicole Bellefontaine[a], Marina A Silveira[c,d], Chelsea N Fortin[b], Thais T Zampieri[d], Jose Donato Jr[e], Kevin W Williams[f], Cristiano Mendes de Silva[g], Laura Heikkinen[h], Christian Broberger[h], Renata Frazao[d], Carol F Elias[a,b*]

*[a]Department of Molecular and Integrative Physiology, [b]Department of Obstetrics and Gynecology University of Michigan, Ann Arbor, MI, 48109. [c]Department of Neuroscience, Developmental and Regenerative Biology, The University of Texas at San Antonio, San Antonio, TX, 78249. [d]Department of Anatomy and [e]Department of Physiology and Biophysics, Institute of Biomedical Sciences, University of Sao Paulo, Sao Paulo, SP, Brazil, 05508. [f]Center for Hypothalamic Research, Department of Internal Medicine, Peter O'Donnell Jr. Brain Institute, The University of Texas Southwestern Medical Center at Dallas, Dallas, TX, 75390. [g]Department of Biosciences, Federal University of Sao Paulo, Santos, SP, Brazil, 11015. [h]Department of Biochemistry and Biophysics, Stockholm University, Stockholm, Sweden.*

*Corresponding Author: Carol F. Elias, Ph.D., North Campus Research Complex B25-3682, 2800 Plymouth Road, Ann Arbor, MI 48109.

cfelias@umich.edu

ORCID iDs:

Cristina Sáenz de Miera: 0000-0001-8047-035X

Marina Augusto Silveira: 0000-0002-8351-5549

Thais T Zampieri: 0000-0002-1611-354X

Jose Donato Jr: 0000-0002-4166-7608

Kevin W Williams 0000-0002-8434-8658

Christian Broberger: 0000-0002-7050-8809

Renata Frazao: 0000-0002-0877-8453

Carol F Elias: 0000-0001-9878-9203

**Key words:** dopamine transporter, leptin, puberty, Kiss1, nutrition, hypothalamus

## Graphical abstract

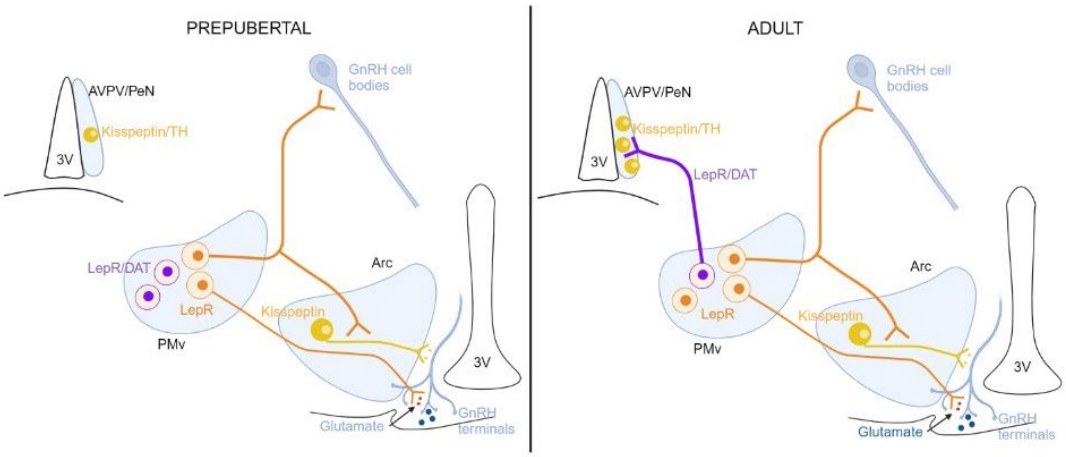


The ventral premammillary nucleus of the hypothalamus plays an essential role in the metabolic control of reproduction. Puberty brings large changes to a subpopulation of $PMv^{LepRb}$ cells expressing the dopamine transporter ($PMv^{DAT}$). DAT gene expression is higher in prepubertal than in adults and is regulated by leptin in prepubertal females. Dynamic projections from $PMv^{DAT}$ cells contact the kisspeptin and tyrosine hydroxylase (TH) populations in the AVPV/PeN during puberty, a critical time for the appearance of these cells in the AVPV/PeN.


## Abstract

Pubertal development is tightly regulated by energy balance. The crosstalk between metabolism and reproduction is orchestrated by complex neural networks and leptin action in the hypothalamus plays a critical role. The ventral premammillary nucleus (PMv) leptin receptor (LepRb) neurons act as an essential relay for leptin action on reproduction. Here, we show that mouse PMv cells expressing the dopamine transporter (DAT) gene, *Slc6a3* ($PMv^{DAT}$) form a novel subpopulation of LepRb neurons. Virtually all $PMv^{DAT}$ neurons expressed *Lepr* mRNA and responded to acute leptin treatment. Electrophysiological recordings from $DAT^{CRE}$;tdTomato mice showed that $PMv^{DAT}$ cells in prepubertal females have a hyperpolarized resting membrane potential compared to diestrous females. *Slc6a3* mRNA expression in the PMv was higher in prepubertal than in adult females. In prepubertal females *Slc6a3* mRNA expression was higher in overnourished females from small size litters than in controls. Prepubertal $Lep^{ob}$ females showed decreased PMv *Slc6a3* mRNA expression, that recovered to control levels after

3 days of leptin injections. Using a tracer adenoassociated virus in the PMv of adult DAT$^{Cre}$;Kiss1$^{hrGFP}$ females, we observed PMv$^{DAT}$ projections in the anteroventral periventricular and periventricular nucleus (AVPV/PeN), surrounding Kiss1$^{hrGFP}$ neurons, a population critical for sexual maturation and positive estrogen feedback in females. The DAT$^{CRE}$;tdTomato projections to the AVPV were denser in adult than in prepubertal females. In adults, they surrounded tyrosine hydroxylase neurons. Overall, these findings suggest that the DAT expressing PMv$^{LepRb}$ subpopulation play a role in leptin regulation of sexual maturation via actions on AVPV kisspeptin/tyrosine hydroxylase neurons.

**Significance Statement**

Women with excess or low energy stores (*e.g.,* obesity or anorexia) have reproductive deficits, including altered puberty onset, disruption of reproductive cycles and decreased fertility. If able to conceive, they show higher risks of miscarriages and preterm birth. The hypothalamic circuitry controlling the interplay between metabolism and reproduction is poorly defined. Neurons in the ventral premammillary nucleus express the leptin receptor and play a key role in the metabolic control of reproduction. Those neurons are functionally and phenotypically heterogeneous. Here we show that a subset of leptin-sensitive neurons co-expresses the dopamine transporter (DAT), is dynamically regulated during pubertal transition and with nutrition and projects to brain sites relevant for sexual maturation.

73 **Introduction**

74 Pubertal development and the maintenance of reproductive function are disrupted in states
75 of negative energy balance or excess energy reserve (1–3). If energy stores are low,
76 puberty is delayed, the reproductive cycles are prolonged, and sub- or infertility ensues
77 (2–4). High adiposity, on the other end, induces earlier pubertal development and
78 decreased fertility in adult life (5–7). The cross-talk between metabolic and reproductive
79 functions is orchestrated by a complex neuronal network modulated by circulating
80 hormones and metabolic cues (8, 9). Among them, leptin has critical roles (10–12). Leptin
81 signaling-deficient subjects develop obesity and remain in an infertile prepubertal state
82 (13–15). In mice, direct leptin actions only in the brain are sufficient to normalize body
83 weight, induce puberty and maintain fertility (10, 14, 16).

84 The ventral premammillary nucleus (PMv) contains a dense collection of leptin receptor
85 (LepRb) neurons, and is recognized as an important hypothalamic site in the metabolic
86 control of reproductive function (4, 16–21). Bilateral lesions of the PMv disrupt estrous
87 cycles and the ability of leptin to increase luteinizing hormone secretion after fasting (4).
88 Endogenous restoration of LepRb exclusively in PMv neurons rescues pubertal
89 maturation and fertility in LepRb *null* female mice (16), while activation of PMv LepRb
90 neurons is sufficient to induce LH release even in normally fed female mice (20). The
91 PMv LepRb neurons, however, do not comprise a homogeneous population, *i.e.,* about
92 75% depolarize and 25% hyperpolarize in response to leptin (22), but their seemingly
93 dissociated nature and function are poorly understood.

94 The PMv neurons are mostly glutamatergic and innervate brain sites associated with
95 reproductive control, sending direct inputs to kisspeptin and gonadotropin-releasing
96 hormone (GnRH) neurons (16, 18, 19, 21, 23). A subset of PMv neurons also expresses
97 the dopamine transporter (DAT), a membrane protein associated with dopamine reuptake
98 at presynaptic terminals (24–26). $PMv^{DAT}$ neurons are unique in the sense that they show
99 seemingly undetectable levels of tyrosine hydroxylase (TH) and dopamine release to
100 specific brain sites (25, 27). Manipulation of $PMv^{DAT}$ neuronal activity has shown an
101 action in male social behavior, inter-male and maternal aggression and maternal
102 behaviors (25, 26, 28, 29). However, the role of $PMv^{DAT}$ neurons in female reproductive

103 physiology has not been described, and whether they participate in the metabolic control
104 of reproductive function is unknown.

105 In this study, we show that DAT is expressed in a subpopulation of $PMv^{LepRb}$ neurons.
106 *Slc6a3* (*DAT*) mRNA expression is higher in prepubertal than in adult females and it is
107 increased in overnourished prepubertal females. We also show that $PMv^{DAT}$ neurons
108 project to and make apparent contacts with kisspeptin neurons in the the anteroventral
109 periventricular nucleus (AVPV) in adults, but not in prepubertal mice.

110 **Methods**

111 ***Experimental animals.*** All procedures were carried out in accordance with the National
112 Research Council Guide for the Care and Use of Laboratory Animals, and protocols were
113 approved by the University of Michigan IACUC (PRO000010420); and in accordance
114 with the European Community Council directive of November 24, 1986 (86/609/EEC)
115 and had received approval by the local ethical board, *Stockholms Djurförsöksetiska*
116 *Nämnd.* Mice were held under a 12h:12h light:dark cycle (lights on at 6 am), temperature-
117 controlled at 21-23 °C, and fed *ad libitum* on a low-phytoestrogen diet (Envigo 2016 diet)
118 and a higher protein and fat phytoestrogen reduced diet 2019 (Envigo 2019 Teklad diet)
119 when breeding. Strains of mice used were a line expressing Cre-recombinase under the
120 *Slc6a3* promoter ($DAT^{Cre}$, JAX®; Stock 006660) (30), and (31) only for female
121 electrophysiology, a ROSA26 stop-floxed tdTomato reporter mouse line (tdTomato,
122 JAX®; Stock 007914), mice expressing GFP under the kiss1 gene promoter: $Kiss1^{hrGFP}$
123 (JAX®, stock 023425) (32), wild type C57B6/J (JAX®; Stock 000664) and the B6.Cg-
124 Lepob/J strain, homozygous mice with an obese spontaneous mutation ($Lep^{ob}$, JAX®;
125 Stock 000632). Adult animals used were postnatal (P) age 60-100 days old, unless
126 otherwise specified.

127 ***Ovariectomy and estradiol replacement.*** To assess the effects of estradiol (E2) on *Slc6a3*
128 gene expression we used ovariectomized (OVX, n=5), OVX + E2 (n=5) and diestrous
129 females (n=4). Females were deeply anesthetized with isoflurane and underwent bilateral
130 OVX. OVX females received steroid replacement via a Silastic capsule containing E2 (1
131 µg, OVX+E2) or oil (OVX) subcutaneously at the time of surgery. OVX females were
132 perfused 7-14 days following surgery, while OVX+E2 females were perfused two days
133 following E2 replacement. Uterus size was used as control for the treatment. Only OVX

134 mice with uterine weight below 80 mg and OVX+E2 mice with uterine weight above
135 100mg were used. Both groups were perfused in the morning to avoid time-of-day effects
136 of estradiol feedback.

137 ***Leptin treatment.*** DAT$^{Cre}$;tdTomato adult (P60-70) males and females fasted overnight
138 and prepubertal (P19) males and females fasted for 4h were intraperitoneally (i.p.)
139 injected with leptin (2.5 mg/kg, National Hormone and Peptide Program, Harbor-UCLA
140 Medical Center, CA) or saline (n=5-6 animals/group). Sixty minutes following leptin
141 injection, mice were perfused with PBS and 10% neutral buffered formalin (NBF, Sigma),
142 brains were postfixed for 2h in 20% sucrose in 10% NBF and stored with 20% sucrose in
143 PBS. 30 µm coronal tissue sections 120 µm apart were processed for pSTAT3
144 immunohistochemistry as described below.

145 Two cohorts of adult wild type females in diestrus i.p. injected with saline, *Lep$^{ob}$* animals
146 i.p. injected with saline (Lep$^{ob}$ + saline) or with leptin (3 mg/kg/day, Lep$^{ob}$ + leptin group,
147 murine leptin, Preprotech), received the treatment for two days at 9 am and 5 pm and one
148 day at 9 am. One hour after the last saline or leptin injection (at 10 am), females were
149 euthanized by decapitation following anesthesia (isoflurane) and brains were harvested
150 and snap frozen. Coronal frozen sections (16 µm) were collected on a cryostat and stored
151 at -80°C until processing for gene expression.

152 ***In situ hybridization (ISH) with radioisotopes.*** Adult wild type (WT) male (n=3) and
153 female (n=4) mice were used to study sex differences in *Slc6a3* gene expression. Female
154 mice were also used to determine developmental differences in *Slc6a3* gene expression,
155 *i.e.,* prepubertal (P19, n=7) *vs.* adult (P60-70, n=5) diestrous mice. To assess the effects
156 of nutritional factors in development on *Slc6a3* gene expression we used P20 females
157 from small litters (SL 2-3 pups/litter, n=5 females) or normal litter (NL 7-9 pups/litter,
158 n=4 females). To assess the effect of leptin in *Slc6a3* expression we used diestrous (n=7),
159 Lep$^{ob}$ + saline (n=5) or Lep$^{ob}$ + leptin (n=5) injected females. Coronal sections were used
160 for radioactive ISH, using an $^{35}$S-UTP or $^{33}$P-UTP labelled *Slc6a3* riboprobe. The
161 following primers were used (exon 10-15 of the *Slc6a3* gene): Forward (5'
162 ACGTCTTGATCACTGGGCTTGTCGATGAGTT 3') and reverse (5'
163 GCATGGATTGGGTGTGAACAGTC 3') to amplify a 754 base-pair sequence in the
164 *Slc6a3* gene (exons 10-15). A clamp sequence followed by sequences for T7

165 (CCAAGCCTTCTAATACGACTCACTATAGGGAGA) and T3
166 (CAGAGATGCAATTAACCCTCACTAAAGGGAGA) promoters were added to the
167 reverse and forward primer sequences, respectively.

168 Single-labeled ISH was performed on 20 µm fresh frozen or 30 µm fixed brain (120 µm
169 distance) sections mounted onto SuperFrost Excell or Superfrost Gold slides (Fisher
170 Scientific). Fixed sections were subjected to a 10-minute microwave sodium citrate (pH
171 6) pre-treatment and hybridized overnight at 57 °C with $^{35}$S-labeled *Slc6a3* riboprobes,
172 as previously described (17, 33). Frozen sections were fixed in ice-cold 10% NBF, treated
173 with 0.25% acetic anhydride and underwent dehydration in ethanol, and hybridized
174 overnight at 57 °C with $^{33}$P-labeled *Slc6a3* riboprobes. All slides were then incubated in
175 0.002% RNase A followed by stringency washes in sodium chloride-sodium citrate buffer
176 (SSC). Slides were exposed to film autoradiography (Kodak), for 3-5 days. Slides were
177 dipped in autoradiographic emulsion (Kodak), dried for 3 hours and stored in light-
178 protected boxes at 4 °C for 2-4 weeks. Slides were developed in D-19 developer,
179 dehydrated in ethanol, cleared in xylene, and coverslipped with DPX (Electron
180 Microscopy Sciences). Film images were acquired using a stereoscope (Zeiss). Darkfield
181 10x images were captured using a digital camera on an AxioImager M2 microscope
182 (Zeiss). ISH signals were quantified using integrated optical density (IOD) in ImageJ
183 software (NIH) using the "freehand" tool to outline the PMv. IOD from the tissue
184 background of the same area was subtracted.

185 ***Fluorescent ISH.*** We used diestrous WT female mice (n=3) to assess *Slc6a3* and *Lepr*
186 mRNA co-expression by fluorescent ISH. ISH was performed on fresh frozen 16-µm
187 thick cryostat sections at 128-µm resolution (8-series). The ISH was performed following
188 the RNAscope protocol for fresh frozen sections, using Protease III (ACDbio, RNAscope
189 Multiplex Fluorescent Reagent Kit v2). Briefly, slides were dried at 60 °C for 15 min,
190 rinsed in PBS for 5 min, fixed in 10% NBF for 15 min at 4 °C, rinsed in PBS-DEPC 2
191 times for 3 min, dehydrated through rinses in serial ethanols for 3 min each, and air-dried
192 for 20 min. A hydrophobic barrier was created around each slide using the ImmEdge pen
193 (Vector Laboratories). The slides were then incubated in $H_2O_2$ for 10 min at RT followed
194 by incubation with Protease III for 30 min at 40 °C. ISH was performed using the
195 RNAscope Protease III (ACDBio). Sections were incubated with Mm-Slc6a3-C1
196 (#315441), and Mm-Lepr-C3 (#402731-C3, labeling all *Lepr* isoforms) RNAscope

197 probes for 2 h at 40°C using the HybEZ Humidifying System (ACDBio). After all
198 incubation steps following the kit's protocol, slides were incubated in DAPI solution for
199 30 s at room temperature, and coverslipped using ProLong Gold Antifade Mountant
200 (ThermoFisher Scientific).

201 Quantification of mRNA coexpression within cells was performed on PMv images
202 acquired with a 40x oil objective on an AxioImager M2 microscope (Zeiss). Based on
203 observed background outside of the area of interest, a threshold for a minimum number
204 of 5 puncta per cell was used to consider a cell positive for expression of that gene.
205 Confocal images were acquired for illustration on a Nikon A1 confocal microscope.

206 ***Electrophysiological recordings.*** Hypothalamic slices from adult DAT$^{Cre}$;tdTomato male
207 (30) and female (31) mice were prepared and the data analyzed as previously described
208 (22). Briefly, mice were decapitated following isoflurane anesthesia, and the entire brain
209 was removed. After removal, the brains were immediately submerged in ice-cold,
210 carbogen-saturated (95% $O_2$ and 5% $CO_2$) artificial cerebrospinal fluid (ACSF, 126 mM
211 NaCl, 2.8 mM KCl, 26 mM $NaHCO_3$, 1.25 mM $NaH_2PO_4$, 1.2 mM $MgSO_4$, 5 mM glucose
212 and 2.5 mM $CaCl_2$). Coronal sections (250 μM) from hypothalamic blocks were cut on a
213 Leica VT1000S vibratome and incubated in oxygenated ACSF at room temperature for
214 at least 1 hour before the recordings. The slices were transferred to the recording chamber
215 and allowed to equilibrate for 10–20 min. The slices were bathed in oxygenated ACSF
216 (32°C) at a flow rate of ~2 mL/min. The pipette solution was in some cases modified to
217 include an intracellular dye (Alexa Fluor 488) for whole-cell recording: 120 mM K-
218 gluconate, 10 mM KCl, 10 mM HEPES, 5 mM EGTA, 1 mM $CaCl_2$, 1 mM $MgCl_2$, 2 mM
219 (Mg)-ATP, and 0.03 mM AlexaFluor 488 hydrazide dye, pH 7.3. Whole-cell patch-clamp
220 recordings were performed on tdTomato-positive neurons anatomically restricted to the
221 PMv. Epifluorescence was briefly used to target the fluorescent cells; at which time the
222 light source was switched to infrared differential interference contrast imaging to obtain
223 the whole-cell recording (Leica DM6000 FS equipped with a fixed stage and a
224 fluorescence digital camera). In current-clamp mode, tdTomato neurons were recorded
225 under zero current injection (I = 0) in whole-cell patch-clamp configuration. The
226 recording electrodes had resistances of 5-7 MΩ when filled with the K-gluconate internal
227 solution. The membrane potential values were compensated to account for the junction
228 potential (-8 mV). In males and females at both ages, the resting membrane potential

229 (RMP) was monitored for at least 10-20 minutes (baseline period) before leptin was
230 administered to the bath. Solutions containing leptin (100 nM) were typically perfused
231 for 15-20 minutes after the baseline period, with a 20-minute washout with ACSF.

232 ***Manipulation of estrous cycles using chemogenetics.*** Adult virgin DAT-Cre females
233 (n=14) received bilateral injection (50 nL/side) of an adenoassociated virus (AAV)
234 expressing a Cre-dependent hM3Dq-mCherry fusion protein,pAAV8-hSyn-DIO-
235 hM3D(Gq)-mCherry (AAV-hM3Dq, Addgene plasmid # 44361, from Bryan Roth) (34)
236 in the PMv using the following coordinates: Anteroposterior = -5.4 mm (from rostral
237 rhinal vein); mediolateral = -0.52 mm (from sagittal sinus); dorsoventral = -5.4 mm (from
238 dura mater). The stereotaxic protocol is described in detail in a previous study (35). One
239 month after surgery, we started to follow the reproductive cycle of these females
240 collecting daily vaginal smears with saline solution. After a period of adaptation, we
241 continued for 13 days with added DMSO (0.0068%) in water, as a control. Next, we added
242 CNO (5 mg/kg) dissolved in DMSO in the drinking water and followed the cycles for 13
243 more days. The abundant presence of cornified cells in the smear was considered as
244 estrus/metestrus, a large abundance of leukocytes was considered as diestrus and a large
245 abundance of nucleated cells with some cornified cells present was considered as
246 proestrus. At the end of the experiment, the females received i.p. injection of CNO and 2
247 h after mice were perfused with PBS and 10% NBF (Sigma), brains were postfixed for 4
248 h in 20% sucrose in 10% NBF and stored with 20% sucrose in PBS. We collected 30 µm
249 coronal tissue sections 120 µm apart. Sections were cryoprotected and frozen until
250 processed to verify the injection sites for these females.

251 ***Tracing PMv-DAT neuronal projections.*** DAT-Cre adult females (n=7) received
252 unilateral stereotaxic injections of an AAV expressing a Cre-dependent
253 channelrhodopsin-mCherry fusion protein (AAV8-hSyn-double floxed-hChR2(H134R)-
254 mCherry, UNC Vector Core, from Karl Deisseroth (Addgene 20297), 25-50 nL) in the
255 PMv. One month after the stereotaxic surgery, mice were perfused with 10% NBF and
256 brains were harvested and processed for histology as above. Fixed coronal 30 µm
257 hypothalamic brain sections were processed for immunofluorescence.

258 ***Immunohistochemistry***. Fixed frozen tissue sections (30 µm at 120 µm distance) from
259 perfused animals obtained with a freezing microtome (Leica) were rinsed in PBS and

260 blocked with PBS + Triton-X 0.25% (PBT) and 3% normal donkey serum (NDS).
261 Primary antibodies were incubated in PBT + 3% NDS overnight at room temperature.
262 Primary antibodies used were Rabbit dsRed antibody (1:5000, Clontech 632496,
263 RRID:AB_10013483), rat monoclonal anti-mCherry 16D7 (1:5000, Invitrogen M11217,
264 RRID:AB_2536611), rabbit anti-cFOS (1:5000, Millipore ABE457,
265 RRID:AB_2631318), chicken anti-GFP (1:10000, Aves GFP-1010,
266 RRID:AB_2307313), rabbit polyclonal anti-GnRH (1:5,000, Phoenix Pharmaceuticals H-
267 003-57, RRID:AB_572248), and sheep anti-TH (1:5000, Millipore AB1542,
268 RRID:AB_90755). For detection of Fos, endogenous peroxidase was blocked with 0.3%
269 $H_2O_2$ for 30 min before the NDS blocking step. For detection of phosphorylation of signal
270 transducer and activator of transcription 3 (pSTAT3), tissue was pre-treated with 1%
271 $H_2O_2$ and with 1% sodium hydroxide in water and then with 0.3% Glycine before
272 blocking with PBT + NDS 3% as before. Tissue was incubated in primary rabbit anti-
273 pSTAT3 (Tyr705) (D3A7) XP® (1:1,000; Cell Signaling 9145S, RRID:AB_2491009) for
274 48 h at 4°C. The corresponding secondary fluorescent antibodies were used for detection
275 (1:500, Invitrogen). For the Fos antibody we performed immunoperoxidase detection
276 using a biotinylated-anti rabbit IgG secondary antibody (1:1000, Jackson
277 Immunoresearch), signal amplification with Avidin Biotin Complex (Vectastain® ABC-
278 HRP Kit, 1:500, Vector labs) for 1 h and signal development with diaminobenzidine
279 (DAB, Sigma) 0.05% and 0.01% $H_2O_2$. Floating sections were then mounted on gelatin-
280 coated slides, dried overnight and coverslipped with Fluoromount-G (Invitrogen).

281 Photomicrographs were acquired using Axio Imager M2 (Carl Zeiss Microscopy).
282 Quantification of pSTAT3, tdTomato and TH positive neurons was performed by an
283 observer unaware of the images' identity. Dual-labeled tdTomato and pSTAT3
284 immunoreactive cells were counted in each individual channel and colocalization was
285 considered where pSTAT3 immunoreactivity (-ir) was clearly nuclear in tdTomato-
286 positive cells. Two sections at the mid-PMv level were counted (~Bregma: -2.46 mm).
287 No correction for double counting was performed because sections were 120μm apart.
288 tdTomato fiber density in the AVPV/PeN was quantified using IOD in ImageJ software
289 (NIH) on both sides of the ventricle in a representative section for each region. An
290 elongated rectangle of the same size for all animals was used as region of interest, placed

291 in contact with the ventricle wall to cover a representative area over the TH-expressing
292 cells.

293 Confocal microscopy images were acquired and analyzed using a Nikon A1 microscope
294 and a Nikon N-SIM + A1R microscope with a resonance scanner.

295 ***Data analysis***. Data are expressed and represented as mean ± SEM. When data did not fit
296 a normal distribution or did not have equal variances, they were transformed to fit a
297 normal distribution and re-analyzed. Unpaired two-tailed Student's t test was used for
298 comparison between two groups. For comparison between three groups, one-way
299 ANOVA was used followed by Tukey's *post-hoc* multiple comparison test. For pSTAT3
300 and %pSTAT3/tdTomato cells, a two-way ANOVA was used with age and sex as factors.
301 Correlation was assessed between body weight and *Slc6a3* gene expression using Pearson
302 R correlation coefficient. A P value less than 0.05 was considered significant. Data were
303 organized and calculated in Excel software (Microsoft, inc.). Statistical analyses and
304 graphs were performed using GraphPad Prism v.9.5 (GraphPad software, inc.). Zen Blue
305 3.7 software (Carl Zeiss Microscopy GmBH) was used to acquire and process
306 epifluorescence images. NIS-elements software (Nikon) was used to acquire and process
307 confocal microscope images. Photoshop 2024 (Adobe, inc.) was used to integrate graphs
308 and digital images into figures. The graphical abstract was prepared using BioRender.
309 Only brightness, contrast, and levels were modified to improve data visualization in the
310 figures.

311 **Results**

312 ***Slc6a3* mRNA expression in the PMv is sexually dimorphic and higher in**
313 **prepubertal females**

314 The *Slc6a3* (DAT) gene is expressed in the PMv of male and female mice (24, 25). To
315 evaluate potential sexual dimorphism or postnatal developmental changes, we assessed
316 *Slc6a3* gene expression in the PMv in adult males and females, and in prepubertal and
317 adult females. PMv *Slc6a3* mRNA levels were higher in diestrous females compared to
318 male mice (n=3 female, n=4 male, unpaired t-test p=0.032 Figure 1A, B, D), and higher
319 in prepubertal females compared to diestrous mice (n=7 prepubertal, n=5 diestrous,
320 unpaired t-test p=0.013 Figure 1B, C, E).

321 To assess if the reduction of PMv *Slc6a3* mRNA in adult female mice is a result of
322 increasing circulating estradiol (E2) during the pubertal transition, hypothalamic sections
323 from diestrous, ovariectomized (OVX), and OVX + E2 mice were analyzed. We found
324 no differences between these groups (n=5 diestrous and OVX+E2, n=4 OVX, one-way
325 ANOVA, $p = 0.54$, Figure 1F).

326 **PMV$^{DAT}$ neurons show heterogenous responses to leptin**

327 We used fluorescent *in situ* hybridization (ISH) to assess transcript coexpression in adult
328 females in diestrus (n=3). Virtually all *Slc6a3* neurons in the PMv coexpressed *Lepr*
329 mRNA (93.1 % ± 1.9), whereas about half of PMv *Lepr* neurons coexpressed *Slc6a3*
330 mRNA (58.6 % ± 4.1, Figure 2A-C).

331 To investigate the effect of leptin on the membrane excitability of PMv$^{DAT}$ neurons, we
332 performed current clamp recordings of DAT$^{Cre}$;tdTomato neurons. In males, the average
333 RMP of recorded neurons was -52.8 ± 2.0 mV (range from -62 to -38 mV, 16 cells from
334 8 mice). In a separate cohort of females, the RMP was -57.2 ± 5.7 mV (range from -62 to
335 -51 mV, 8 cells from 6 mice). We found that bath application of 100 nM leptin
336 hyperpolarized 25% of the recorded neurons of male mice (4/16 cells Figure 2D-G). The
337 RMP of the remaining 75% of the recorded cells was unchanged or showed a continuous
338 depolarizing trend and were removed from the analysis. In females in diestrus, ~75% (6/8)
339 of recorded cells hyperpolarized in response to bath application of 100nM leptin (Figure
340 2G). Two PMv$^{DAT}$ neurons showed a depolarizing response and one showed continuous
341 depolarization and was removed from the analysis (Figure 2E). The leptin-associated
342 hyperpolarization of PMv$^{DAT}$ cells was of similar amplitude in both sexes: -7.8 ± 0.8 mV
343 in males, and -6.3 ± 2.0 mV in females.

344 Although most (> 90%) of *Slc6a3* expressing neurons express *Lepr*, only a subpopulation
345 exhibits a response, including both de- and hyperpolarization, in electrical properties to
346 the hormone.

347 **Long-term activation of PMv$^{DAT}$ neurons does not alter estrous cycles in adult**
348 **virgin females**

349 Given the higher percentage of female's DAT$^{Cre}$;tdTomato neurons that are
350 hyperpolarized by leptin, we decided to investigate if long-term activation of these
351 neurons might impair the reproductive cycle of the adult females. We stereotaxically

352 injected the AAV-hM3Dq virus bilaterally in the PMv of 14 DAT$^{Cre}$;tdTomato virgin
353 females. Twelve females had bilateral injections and one had a unilateral injection
354 centered in the PMv, defined by the expression of mCherry and Fos immunoreactivity
355 that indicates they had been activated by CNO (Figure 3A-B). Two animals had missed
356 injections with not Cherry expression observed in either PMv, and lack of Fos confirmed
357 in the PMv of these animals (Figure 3C). Of the twelve animals with bilateral injection,
358 eleven showed regular cycling (at least two complete cycles) during the control (DMSO)
359 period and were used for the analyses (Figure 3D). The cycles of the bilaterally injected
360 females were not altered by the CNO when compared to the DMSO exposure (paired t-
361 test DMSO *vs*. CNO, days in estrus/metestrus, p=0.59; days in diestrus, p=0.68; cycle
362 length, p=0.69, n=11, Figure 3E-G). We paid special attention to the potential virus spread
363 to a nearby population of *Slc6a3* expressing cells, the tubero-infundibular dopamine
364 (TIDA) neurons in the arcuate nucleus (Arc), (24). Six mice showed some viral
365 contamination of TIDA neurons, but no differences in cyclicity or cycle length were
366 noticed when these animals were removed from the analysis. These results suggest that
367 these cells have no effect on female cyclicity.

368

369 **Prepubertal PMv$^{DAT}$ neurons respond to leptin and show distinct membrane**
370 **properties compared to adult females.**

371 Due to increased expression of *Slc6a3* in prepubertal females, we explored the functional
372 response of PMv$^{DAT}$ neurons to exogenous leptin. Adult and prepubertal
373 DAT$^{Cre}$;tdTomato mice received an i.p. injection of leptin, and one hour after,
374 colocalization of pSTAT3-ir in tdTomato neurons was quantified. No differences were
375 observed in the number of pSTAT3-ir cells with age or sex in leptin treated mice (n = 3-
376 5; Two-way ANOVA, p=0.28 for Sex; p=0.79 for Age; Figure 4A-G). Virtually no
377 pSTAT3-ir was observed in the PMv of saline treated mice (n=5 per group). As expected
378 from the *Slc6a3* and *Lepr* coexpression data, 95.3 – 99.3 % of tdTomato neurons in the
379 PMv colocalized with pSTAT3-ir in adults of both sexes (Figure 4H). Similar
380 colocalization was observed in prepubertal mice of both sexes (96.4 – 98.9 %, Figure 4H).
381 About 30% of PMv pSTAT3-ir neurons colocalized with tdTomato in females (25.9 ±

382 2.8% prepubertal, and 33 ± 2.4% in diestrous, p=0.14) and males (27.8 ± 1.8%
383 prepubertal, and 35.6 ± 4.8% in adults, p=0.18).

384 When examined by electrophysiology, the $PMv^{DAT}$ neurons of prepubertal (unweaned)
385 female mice revealed heterogeneous properties. Interestingly, the RMP of prepubertal
386 $PMv^{DAT}$ neurons was more hyperpolarized compared to adult diestrous females (n=8
387 prepubertal and n=8 diestrous, unpaired t-test, p <0.0001, Figure 4I). In response to leptin
388 treatment, three out of eight cells (37.5%) from three mice showed no RMP change and
389 another three out of eight cells (37.5%) responded by hyperpolarization (Figure 4J). Two
390 out of eight cells (25%) depolarized after acute leptin, but none of them recovered after
391 washout. Two recorded cells showed continuous depolarization and were removed from
392 the analysis. The hyperpolarized cells showed a -6.3 ± 2.1 mV change in the RMP after
393 treatment.

394 Our findings indicate that the $PMv^{DAT}$ neuron population from prepubertal (unweaned)
395 female mice is in a less excitable state compared to adult mice.

396 **Postnatal overnutrition increases *Slc6a3* mRNA expression in the PMv of**
397 **prepubertal females**

398 We next assessed if the expression of *Slc6a3* mRNA is altered in the PMv of leptin
399 deficient $Lep^{ob}$ infertile female mice, which remain in a prepubertal state. We employed
400 a paradigm of leptin treatment and pubertal progression in which $Lep^{ob}$ females were
401 injected with saline or leptin twice a day for 2 ½ days are compared to age-matched wild
402 type diestrous females (16, 36). As expected, the leptin-treated $Lep^{ob}$ mice showed a
403 significant decrease in body weight and displayed signs of pubertal progression (vaginal
404 opening) following the leptin treatment. We found that *Slc6a3* mRNA expression is ~40%
405 lower in non-treated $Lep^{ob}$ females, compared to wild type females in diestrus (n=5-7;
406 p=0.0025 one-way ANOVA, Tukey's *post-hoc*, p=0.005 Figure 5A). The short-duration
407 leptin treatment regimen was sufficient to induce a ~ 40% increase in *Slc6a3* mRNA
408 expression in the PMv of $Lep^{ob}$ mice (Tukey's *post-hoc*, p=0.005, Figure 5A),
409 concomitant with the first signs of puberty onset.

410 Given the complex phenotype of the $Lep^{ob}$ mouse (37), we employed a paradigm of
411 postnatal overnutrition, which leads to high leptin levels and early puberty (38, 39). We
412 compared *Slc6a3* mRNA expression in the PMv of females raised in normal (NL, n=4

413 females) versus small (SL, n=5 females) litter sizes. Body weight was higher in SL
414 offspring as compared to NL (9.67 ± 0.59 g in SL *vs*. 5.65 ± 0.39 g in NL, unpaired t-test
415 p=0.001). *Slc6a3* mRNA levels were higher in the SL than in those in NL (p=0.007,
416 Figure 5B-D) and were strongly correlated to body weight (Pearson r=0.78; p=0.01,
417 Figure 5E).

418 ***PMv$^{DAT}$ neurons project to kisspeptin AVPV/PeN neurons***

419 To assess if PMv$^{DAT}$ neurons are part of the circuitry regulating pubertal development,
420 DAT$^{Cre}$; *Kiss1$^{hrGFP}$* females were unilaterally injected with a Cre-dependent AAV
421 expressing a channelrhodopsin-mCherry fusion protein (AAV-ChR2-mCherry) into the
422 PMv (n=7). Abundant mCherry-ir neurons were observed within the PMv in correctly
423 targeted animals (n=6). Mice showing virus spread to nearby DAT expressing populations
424 were removed from the analysis (n=2 were analyzed, Figure 6A). In accordance with
425 previous studies focused on PMv projections (41, 42), dense mCherry-ir fibers were
426 found in several hypothalamic regions including the AVPV (Figure 6B), the
427 periventricular nucleus (PeN) the medial preoptic area (MPA, Figure 6C), and the
428 ventrolateral subdivision of the ventromedial hypothalamus (VMHvl, not shown). Most
429 notably, very sparse innervation of the Arc was observed (Figure 6D). No mCherry-ir
430 projections were observed nearby or in contact with GnRH cell bodies in the medial
431 septum (MS) or MPA (not shown).

432 To explore a possible interaction of PMv$^{DAT}$ neurons with kisspeptin, we analyzed
433 mCherry-ir fibers in proximity to *Kiss1$^{hrGFP}$* cells using confocal microscopy. As
434 expected, due to the low innervation of the Arc, kisspeptin/neurokinin 3/dynorphin
435 (KNDy) neurons did not receive close appositions from PMv$^{DAT}$ neurons (Figure 6E). In
436 contrast, dense mCherry innervation of kisspeptin cells was observed in the AVPV and
437 PeN region (AVPV/PeN, a.k.a. rostral periventricular area of the third ventricle, Figure
438 6F) of the adult female mouse.

439 ***PMv$^{DAT}$ innervation of AVPV/PeN is established during the pubertal transition***

440 The AVPV/PeN area contains a sexually dimorphic population of dopaminergic TH and
441 kisspeptin cells, both denser in females. About 50-90% of the *Kiss1* cells express TH in
442 mice (40–43), and kisspeptin expression in this region increases during the pubertal
443 transition (40, 44). In DAT$^{Cre}$;tdTomato mice, we found that AVPV/PeN TH neurons do

444 not express tdTomato. DAT$^{Cre}$;tdTomato fiber density was about three times higher in the
445 AVPV (p=0.006, Figure 7A, B and E), and about ten times higher in the PeN of adult *vs*.
446 prepubertal females (p=0.003, Figure 7C, D and E). As observed for *Kiss1*, the number
447 of neurons expressing TH was higher in both the AVPV and the PeN of adult diestrous
448 female mice compared to prepubertal females (p<0.0001 in the AVPV; p<0.0001 in the
449 PeN, Figure 7A-D, F). DAT$^{Cre}$;tdTomato terminals were in close apposition to TH
450 neurons and fibers in the AVPV/PeN of adult female mice (Figure 7G-H).

451 **Discussion**

452 The present study revealed a novel subset of leptin responsive cells within the PMv that
453 show dynamic regulation of the *Slc6a3* (DAT) mRNA during puberty and specific
454 projections to hypothalamic sites and neurons involved in puberty and reproductive
455 control. The overall PMv$^{Leprb}$ population is key in the metabolic regulation of puberty and
456 fertility, whereas the PMv$^{DAT}$ neurons were previously shown to be involved in
457 aggression, social and maternal behaviour (25, 26, 28, 29). Our findings indicate that the
458 PMv$^{DAT}$ population represents a discrete subset of PMv$^{LepRb}$ neurons and a novel
459 candidate for mediating nutritional modulation of reproduction and pubertal
460 development.

461 Within the PMv, leptin-induced pSTAT3 was observed in all DAT-expressing cells.
462 However, acute leptin exposure had heterogenous sex- and age-dependent effects on the
463 excitability of DAT$^{Cre}$ neurons. The lack of electrophysiological response of a
464 subpopulation suggests that these neurons are responsive to leptin in ways not tested in
465 this study, *e.g.* by means of transcriptional regulation. Acute leptin action in the PMv$^{Leprb}$
466 population is also heterogenous, inducing the depolarization of 75% of these cells, via a
467 putative transient receptor potential channel (TRPC) channel, and hyperpolarizing 25%
468 cells, via activation of a putative Katp channel, while no cells were found to be
469 unresponsive to the treatment (22). Importantly, the RMP of prepubertal females was
470 more hyperpolarized than that of adult females suggesting that these cells may increase
471 in excitability with maturation and only assume a more active role within the circuit after
472 puberty. PMv$^{DAT}$ cells are responsive to prolactin and oxytocin (29, 45) and the influence
473 of these hormones may contribute to switching these cells from a quiescent to an excitable
474 state in their role in maternal aggression (29). Further studies are needed to determine the

475 acute and chronic effects of leptin on the electrical properties of PMv$^{DAT}$ neurons in
476 distinct developmental and physiological states, as well as the mechanisms associated
477 with changes in intrinsic physiological properties of PMv$^{DAT}$ neurons from prepubertal to
478 adults.

479 PMv$^{DAT}$ cells have been described as a non-dopaminergic population (25, 27). These cells
480 are an active glutamatergic population and send excitatory inputs to projection sites, in
481 particular the VMHvl (25, 26). Several studies, including ours (not shown) have observed
482 a lack of TH expression in this population (27, 46). Only one study has shown an
483 enrichment in TH using Ribotag mice, but to a much lower extent than classical midbrain
484 dopaminergic cells (25). Still, PMv$^{DAT}$ neurons express other elements of the
485 dopamine/monoamine regulation pathway, such as *Gucy2c*, *Aadc* and *Vmat2* (25, 47). In
486 shrews, dopamine and serotonin have been detected in the PMv after L-DOPA and 5-
487 HTP treatment, respectively (47). However, in mice studies using fast-scan cyclic
488 voltammetry have suggested that PMv$^{DAT}$ neurons do not produce dopamine, even when
489 supplemented with L-DOPA (25). Thus, a significant role for dopamine release from
490 these neurons is viewed as unlikely. Still, here we have discerned differences in the
491 regulation of the dopamine transporter that merit further attention.

492 *Slc6a3* mRNA expression in the PMv was higher in females than in males, and showed a
493 developmental decrease after puberty, suggesting a regulation during sexual maturation.
494 Removal of the ovaries or changes in estrogen levels did not affect *Slc6a3* mRNA
495 expression, making estrogen an unlikely regulator during the pubertal shift. Leptin is
496 critical for puberty and fertility. Here, overnourished prepubertal animals from SL
497 showed increased level of *Slc6a3* mRNA expression in PMv, correlated with individual's
498 body mass, although other factors, such as altered sex distribution in the mostly-females
499 SL could also affect gene expression. Furthermore, the rescue of *Slc6a3* mRNA levels
500 observed in leptin-treated *Lep$^{ob}$* animals suggests that leptin has an active role in
501 increasing *Slc6a3* gene expression during pubertal transition. Whether other hormones
502 (*e.g.* prolactin, oxytocin), different physiological states or social behaviors affect PMv
503 *Slc6a3* expression is unknown.
504 Leptin regulation of dopaminergic neurotransmission in the midbrain (substantia nigra
505 and ventral tegmental area) is involved in motivation for food rewards and locomotion
506 (48–50). Leptin specifically regulates dopamine-related genes in these populations (51)

507 and their action in the nucleus accumbens (52). It is important to note though that most
508 studies investigating the role of PMv neurons have used DAT-Cre mice as a strategy to
509 assess the PMv's neuronal function and circuitry, not DAT expression and function. More
510 studies are needed to reveal the role of dopamine-related genes in the PMv, but our
511 findings suggest that *Slc6a3* and its regulation by leptin have a role in pubertal maturation.
512 DAT is mostly found in presynaptic terminals (53); so, this role might be relevant in PMv
513 projection sites, perhaps regulating the neurotransmission of PMv neurons.

514 The $PMv^{DAT}$ neurons project to a subset of brain sites innervated by the $PMv^{Leprb}$
515 population. The $PMv^{Leprb}$ population innervates VMHvl, and key neuronal populations in
516 the control of reproduction, namely, GnRH neurons in the OVLT, MPA and medial
517 septum areas, KNDy neurons in the Arc, and kisspeptin cells in the AVPV/PeN (16, 18,
518 54). As reported before, $PMv^{DAT}$ neurons project to the VMHvl and the supramammillary
519 nucleus (25, 26). In the MPA, we observed little density of axons. However, we observed
520 a very dense collection of terminals in the AVPV/PeN. Differences with previous studies
521 might arise from the use of a different protein marker (ChR2 *vs*. synaptophysin). Of the
522 reproductive populations targeted by $PMv^{Leprb}$ neurons, the $PMv^{DAT}$ neurons seem to
523 specifically target the kisspeptin population in the AVPV/PeN. These results show that
524 the $PMv^{DAT}$ subpopulation target a group of neurons essential for pubertal development
525 in females, supporting a function in puberty.

526 In adults, AVPV/PeN kisspeptin neurons mediate the positive feedback action of estradiol
527 on LH surge that precedes ovulation on the afternoon of proestrus (55). We recently
528 showed that acute activation of the $PMv^{Leprb}$ population in females leads to LH release
529 (20). However, chronic chemogenetic activation of $PMv^{DAT}$ cells had no effect on estrous
530 cycles (present study). Alterations of the LH surge in proestrus have been observed in the
531 absence of effects on estrous cycle progression (56). Therefore, we cannot discard any
532 effects on the LH surge, which can be disrupted after PMv lesions in rats (4, 57). The lack
533 of direct $PMv^{DAT}$ projections to Arc KNDy or GnRH neurons, the dynamic changes in
534 *Slc6a3* expression and neuronal properties, the dense projections to the AVPV/PeN, and
535 the AVPV/PeN's intense chemical remodelling during puberty maturation, suggest that
536 the $PMv^{DAT}$ population could undergo a functional switch during pubertal maturation. We
537 hypothesize that the $PMv^{DAT}$ population could play an important role in the regulation of

538 sexual maturation and later reproductive function, integrating the nutritional state from
539 leptin signal into the AVPV/PeN.

540 Similar to gene expression, the innervation of the AVPV/PeN from $DAT^{Cre}$ neurons was
541 dynamically regulated during female puberty. In adult females DAT projections densely
542 englobed TH neurons, a trait absent in prepubertal females. This timing probably reflects
543 an increase in *Slc6a3*-driven *Cre* expression and a delay to observe tdTomato -ir. The
544 AVPV is a sexually dimorphic population, with higher cell abundance in the female (58).
545 Similar to kisspeptin neurons, the TH population in the AVPV/PeN is sexually dimorphic,
546 with more cells present in females (59, 60).

547 Notably, TH expression in the AVPV/PeN was much lower in prepubertal females than
548 in the adults, a similar developmental time as kisspeptin appearance (61) and the increase
549 of DAT terminals in the AVPV/PeN. This is significant because the AVPV/PeN region
550 is one of the classical dopaminergic regions of the hypothalamus, also known as A15 area
551 (62). The A15 TH neurons do not express DAT (46, 63, 64). Prototypical dopaminergic
552 neurons (*i.e.,* in the midbrain), co-express TH and DAT, so that dopamine is recycled by
553 DAT at the presynaptic terminal. The significance of our current finding is puzzling.
554 However, a recent report provided evidence that DAT plays an integral role in managing
555 the dopaminergic micro-circuitry within the ARH TIDA neurons (65), suggesting that
556 $PMv^{DAT}$ could participate in the AVPV/PeN dopamine microcircuitry, potentially via
557 expression of Aromatic l-aminoacid decarboxylase (AADC) (25, 47). We therefore
558 speculate that the presence of DAT at the PMv presynaptic terminal plays a role in
559 regulating dopaminergic tone in the AVPV/PeN microcircuits and female reproductive
560 function. In addition, $PMv^{DAT}$ neurons likely act on AVPV cells via glutamatergic
561 signaling. AVPV TH neurons play a role in maternal behavior and intermale aggression
562 (66). Whether the $PMv^{DAT}$ neurons' action in the same social behaviors is associated with
563 AVPV/PeN TH neuronal innervation has not been determined.

564 Our present findings demonstrate that the role of PMv neurons in regulating reproductive
565 physiology is more complex than previously anticipated. While overall $PMv^{Leprb}$ neurons
566 play a significant role in female reproduction, particularly mediating leptin's permissive
567 effects in puberty (16), $PMv^{DAT}$ cells have been studied primarily in the context of social
568 behavior and aggression (25, 26, 28, 29). The dynamic changes observed in *Slc6a3* gene

expression during puberty and in response to nutrition, as well as the developmental difference in the innervation of kisspeptin/TH neurons of AVPV/PeN, suggest that the $PMv^{DAT}$ neurons also play a role in sexual maturation.

**Acknowledgements**

We thank Dr. Yun-Hee Choi for the design of the DAT riboprobe, and Susan Allen for expert technical assistance. This work was supported by the National Institutes of Health (R01-HD-069702 to CFE, CSM and NB, R21 HD109485 to CFE and CSM), Michigan Nutrition and Obesity Research Center (URM Pilot Grant P30 DK089503 to CSM) CNPq (Brazilian National Council for Scientific and Technological Development fellowship to BCB), the Knut and Alice Wallenberg Foundation (2020.0054) and the Swedish Research Council Distinguished Professorship Grant (2021-00671) to CB, the Coordenação de Aperfeiçoamento de Pessoal de Nível Superior – Brasil (CAPES) – Finance Code 001 (MAS) and by the São Paulo Research Foundation [FAPESP-Brazil, grants number: 13/07908-8 (RF), 15/20198-5 (TTZ) and the National Institutes of Health (R01 DK119169, R56 DK135501, and PO1 DK119130-03 to KWW).

**Figure Legends**

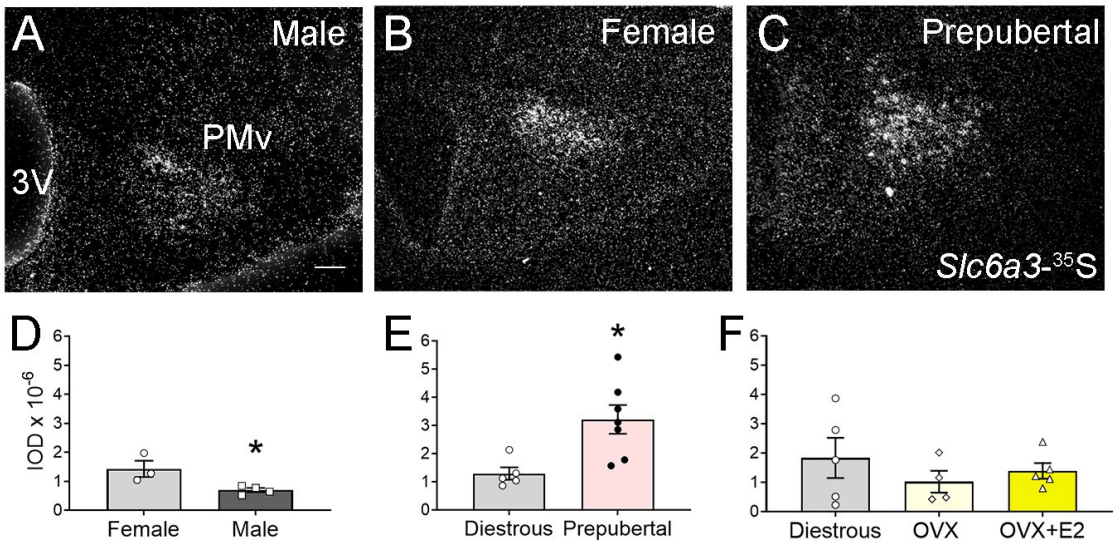


**Figure 1. Ventral premammillary nucleus (PMv) *Slc6a3* gene expression varies with sex and development. A-C.** Darkfield images showing the *Slc6a3*-$^{35}$S hybridization signal (silver grains) in the PMv of adult male, a diestrous female and a prepubertal female, respectively. **D-F.** Graphs showing the quantification of the *Slc6a3*

590 hybridization signal in adult male *vs*. diestrous females, in prepubertal *vs*. diestrous
591 females and in diestrous *vs*. ovariectomized (OVX) females and OVX females
592 supplemented with estradiol (E2). Scale bar = 100 µm. * p<0.05.

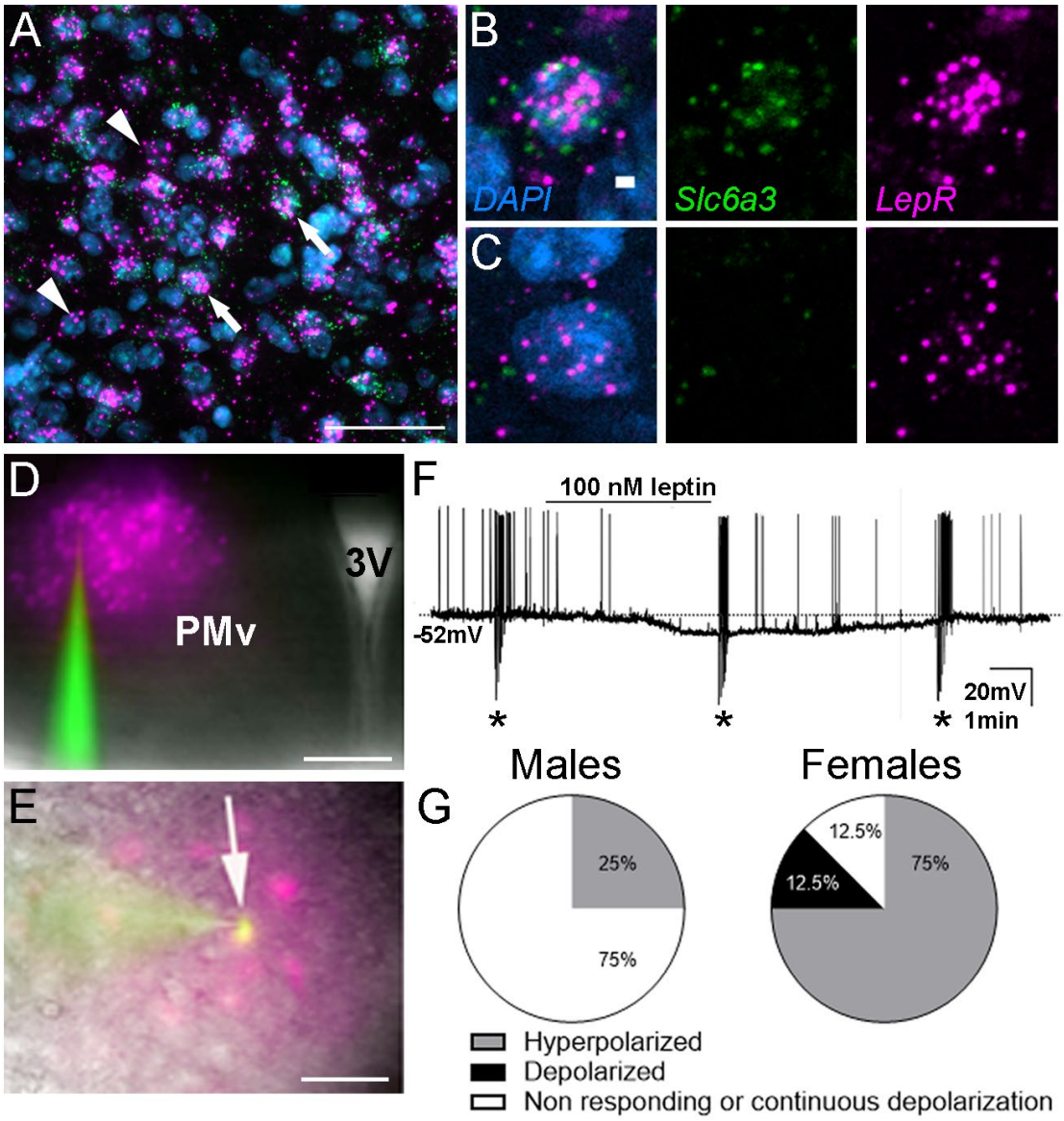


593

594 **Figure 2. A subpopulation of leptin receptor (*Lepr*) expressing neurons in the**
595 **ventral premammillary nucleus (PMv) co-expresses dopamine transporter**
596 **(*Slc6a3*). A.** Fluorescent image showing representative fluorescent *in situ* hybridization
597 depicting the colocalization of *Lepr* (magenta) and *Slc6a3* (green) in the PMv of a
598 diestrous female. Arrows point to cells co-expressing *Lepr* and *Slc6a3* mRNA.
599 Arrowheads point to cells expressing only *Lepr*, but not *Slc6a3*, mRNA. Blue = DAPI.
600 **B-C.** Higher magnification of individual cells depicted in A that co-express *Slc6a3* and

601 *Lepr* mRNA (B), and of a cell that expresses only *Lepr* mRNA (C). **D.** Fluorescent
602 image showing the PMv in the brain slices, recognized by tdTomato expression in
603 DAT$^{Cre}$ neurons. **E.** Merged image showing the colocalization between a recorded
604 DAT$^{Cre}$;tdTomato neuron (magenta) and the AF488 dye (green), dialyzed during the
605 recording. **F.** Representative current-clamp recording demonstrating leptin (100 nM)
606 induced hyperpolarization in a subset of DAT-Cre tdTomato neurons of a male mouse.
607 The dashed line indicates resting membrane potential (-52 mV). Asterisks indicate
608 square pulse current injections to assess input and access resistance. **G.** Pie charts
609 representing the percentage of neurons that hyperpolarized, depolarized or did not
610 respond to 100nM leptin in adult males (N=16) and in adult diestrous females (N=8).
611 Scale bars: A and E = 50 µm, B-C: 2 µm, D= 400 µm.

612

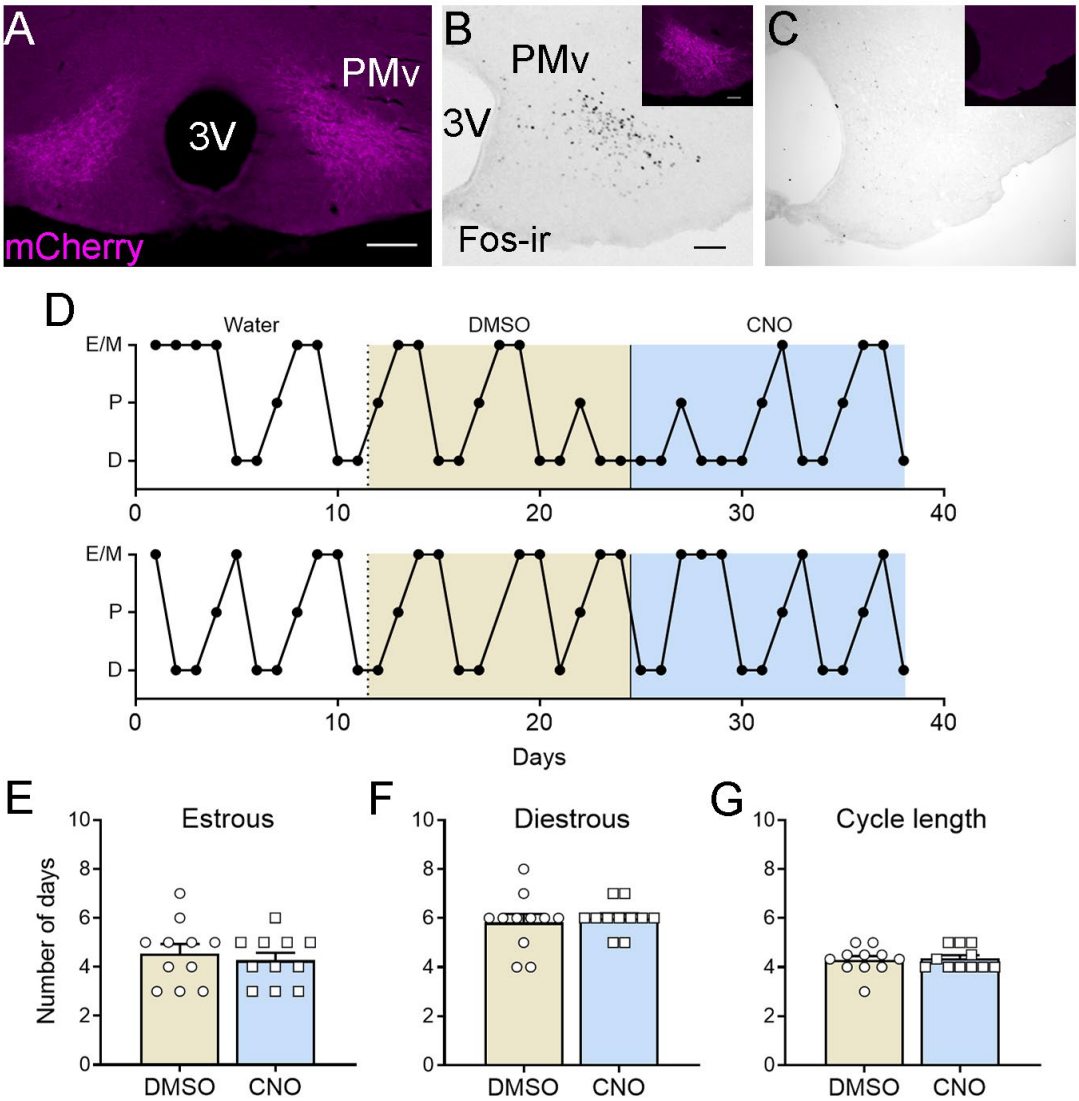


613

614 **Figure 3. Continuous activation of dopamine-transporter neurons in the ventral**
615 **premammillary nucleus (PMv$^{DAT}$) does not alter estrous cycles in adult DAT$^{Cre}$**
616 **female mice. A.** Representative low-magnification fluorescent image of bilateral
617 injections of adenoassociated virus (AAV) expressing Cre dependent hM3Dq-mCherry
618 targeted to the PMv of a female DAT$^{Cre}$ mouse. **B.** High magnification image showing
619 Fos immunoreactivity (Fos-ir) in one PMv side following an intraperitoneal injection of
620 clozapine-N-oxide (CNO) and corresponding fluorescent image of the PMv showing
621 mCherry immunofluorescence. **C.** High magnification image showing the lack of Fos-ir
622 in one PMv side of a missed AAV injection, following an intraperitoneal injection of
623 clozapine-N-oxide (CNO) and corresponding fluorescent image of the PMv showing the
624 lack of mCherry immunofluorescence. **D.** Representative estrous cycles of two females

with AAV injections centered in the PMv before treatment (drinking water), during the treatment with DMSO (vehicle) and CNO in drinking water. E/M: estrus/metestrus; P: Proestrus; D: Diestrus. **E-G.** Graphs showing the number of days spent in estrus/metestrus, diestrus and the cycle length (number of days) in the DAT$^{Cre}$ females with bilateral PMv AAV-hM3Dq injections during the DMSO and the CNO treatment.

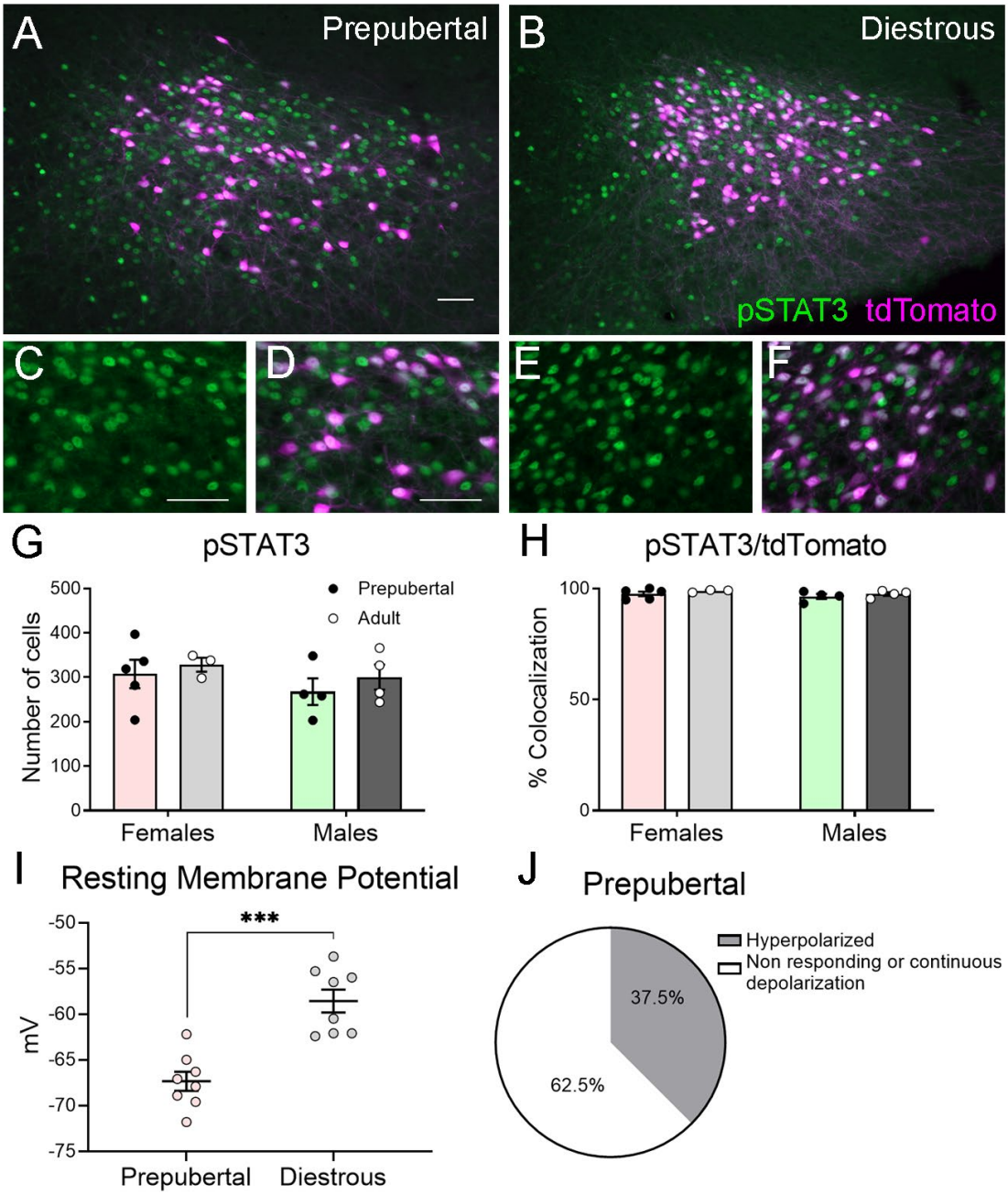

632 **Figure 4. Prepubertal dopamine-transporter neurons in the ventral**
633 **premammillary nucleus (PMv$^{DAT}$) are responsive to leptin but are more**
634 **hyperpolarized than in adult females.**

635 **A, B.** Fluorescent images showing the colocalization of pSTAT3 (green) and tdTomato
636 (magenta) immunoreactivities in the PMv of prepubertal and adult diestrous
637 DAT$^{Cre}$;tdTomato females 1h after a 2.5 mg/kg intraperitoneal leptin injection. **C-F**:
638 High magnification images of the images depicted in A (C, D) and B (E, F). **G, H.**
639 Graphs showing the number of pSTAT3 neurons per section (G) and the percentage of
640 tdTomato cells expressing pSTAT3 (H) in the PMv of prepubertal and adult
641 DAT$^{Cre}$;tdTomato female mice. Prepubertal (n=5) and diestrous (n= 3) females,
642 prepubertal and adult males (n=4 each). **I.** Graph showing the resting membrane
643 potential of individual cells from prepubertal and adult females (n=8 each). ***
644 $p<0.001$. **J.** Pie chart representing the percentage of neurons that hyperpolarized or did
645 not show a change in membrane potential to 100nM of leptin in prepubertal females
646 (N=8). Scales in A-B = 50 µm. C-F = 20 µm.

647

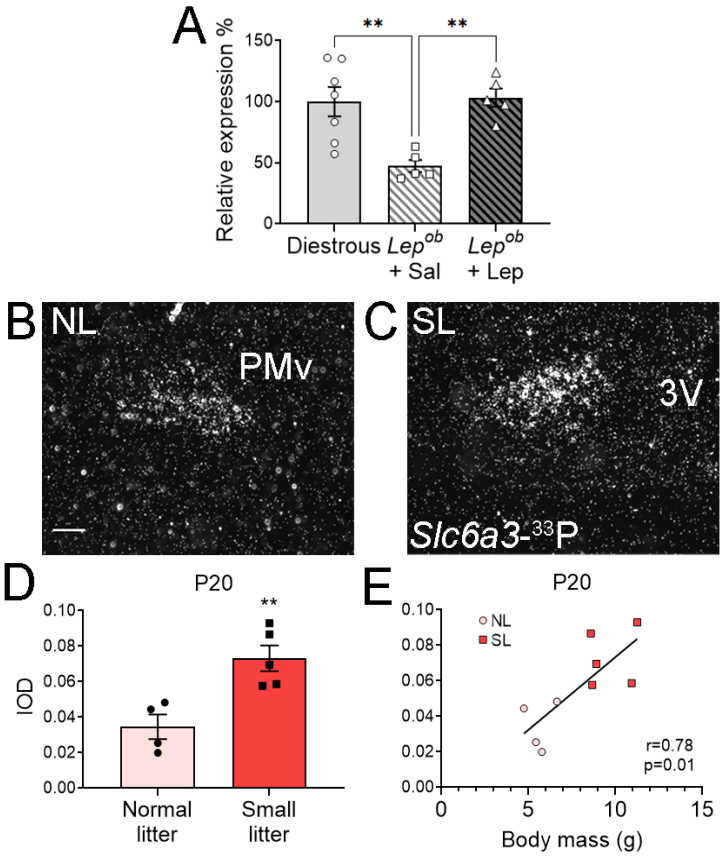


648

649 **Figure 5. *Slc6a3* (DAT) gene expression in the ventral premammillary nucleus**
650 **(PMv) of prepubertal mice is affected by nutrition and leptin. A.** Graph showing the
651 quantification of *Slc6a3*-$^{33}$P hybridization signal as relative expression (%) in diestrous
652 wild type *vs*. prepubertal *Lep$^{ob}$* females injected with saline or with leptin. n=7 for
653 diestrous and for *Lep$^{ob}$* + saline, n = 5 for *Lep$^{ob}$* + leptin. **B-C.** Dark-field images
654 showing the *Slc6a3*-$^{33}$P hybridization signal (silver grains) in the PMv of prepubertal
655 females (P20) from normal litter (NL) size (B) and from small litter (SL) size (C). **D.**
656 Graph showing the quantification of the *Slc6a3* hybridization signal (integrated optic
657 density) in P20 females from normal and small size litters. n=4 animals for normal litter
658 and n = 5 animals for small litter. **E.** Graph showing the correlation between female
659 body mass and the *Slc6a3* hybridization signal (IOD) in P20 females from normal and
660 small size litters. Scale bar in B = 100 µm. ** $p<0.01$.

661

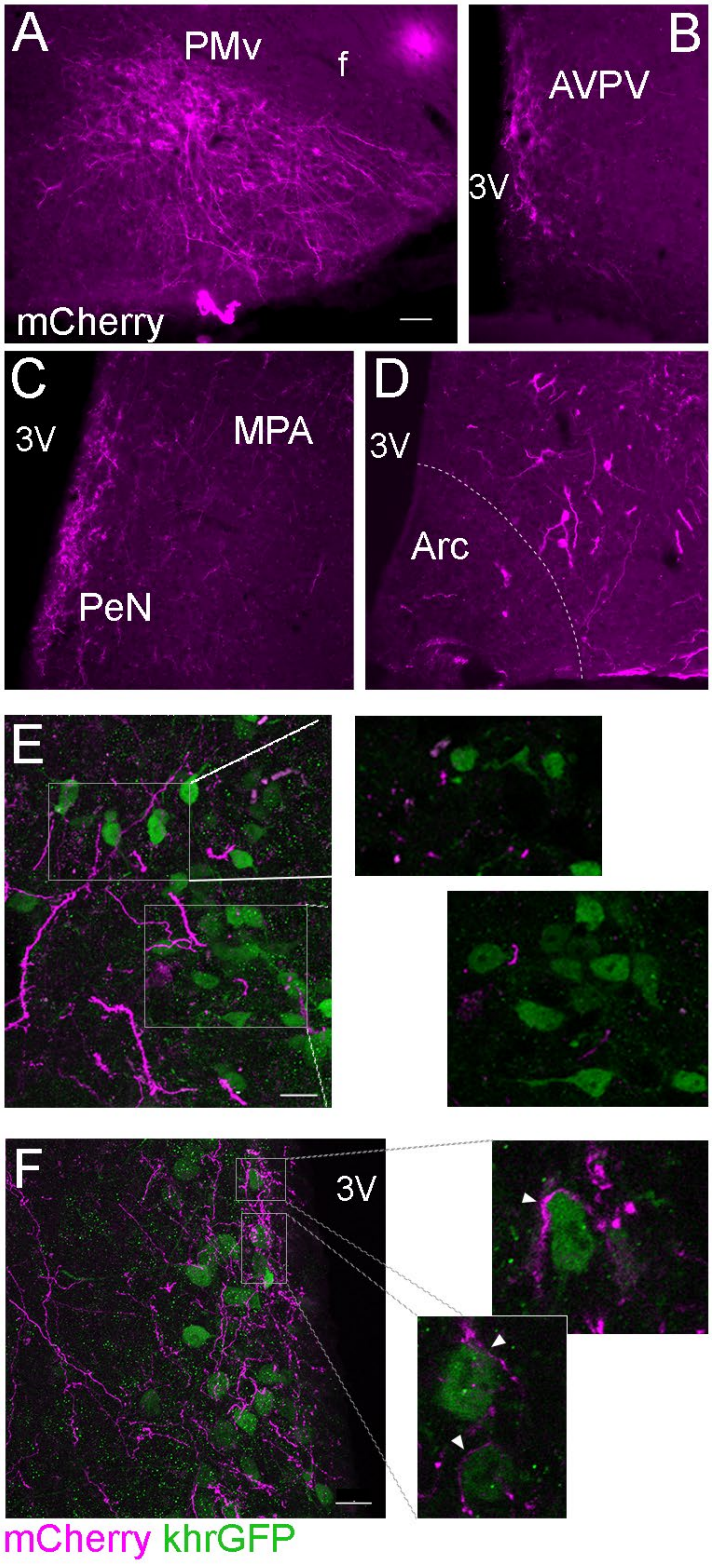


662

663 **Figure 6. Dopamine-transporter neurons in the ventral premammillary nucleus**
664 **(PMv$^{DAT}$) project to the AVPV and PeN and contact kisspeptin neurons. A-D**.
665 Fluorescent image showing ChR2-mCherry signal at the site of the injection in the PMv

666 A, and the projections to the Anteroventral periventricular nucleus (AVPV, B), the
667 Periventricular nucleus (PeN) and the Medial preoptic area (MPA, C), and presence of
668 few projections in the arcuate nucleus (Arc, D). **E.** Confocal fluorescent maximum
669 intensity projection image showing the lack of mCherry (magenta) projections close to
670 kisspeptin (*kiss1*hrGFP, khrGFP) neurons (green) in the Arc. Insets are higher
671 magnification single z plane images showing detail of mCherry signal in the external
672 part of the dorsal Arc and the lack of contacts to khrGFP neurons in this area. **F.**
673 Confocal fluorescent maximum intensity projection image showing mCherry signal
674 (magenta) in the AVPV/PeN and the intense interaction of these projections to khrGFP
675 neurons (green) in this area. are higher magnification single z plane images showing
676 detail of the close contacts between these two populations (arrowheads). f: fornix; 3V:
677 Third ventricle. Scale bar A-D = 50 µm. E-F = 20 µm.

678

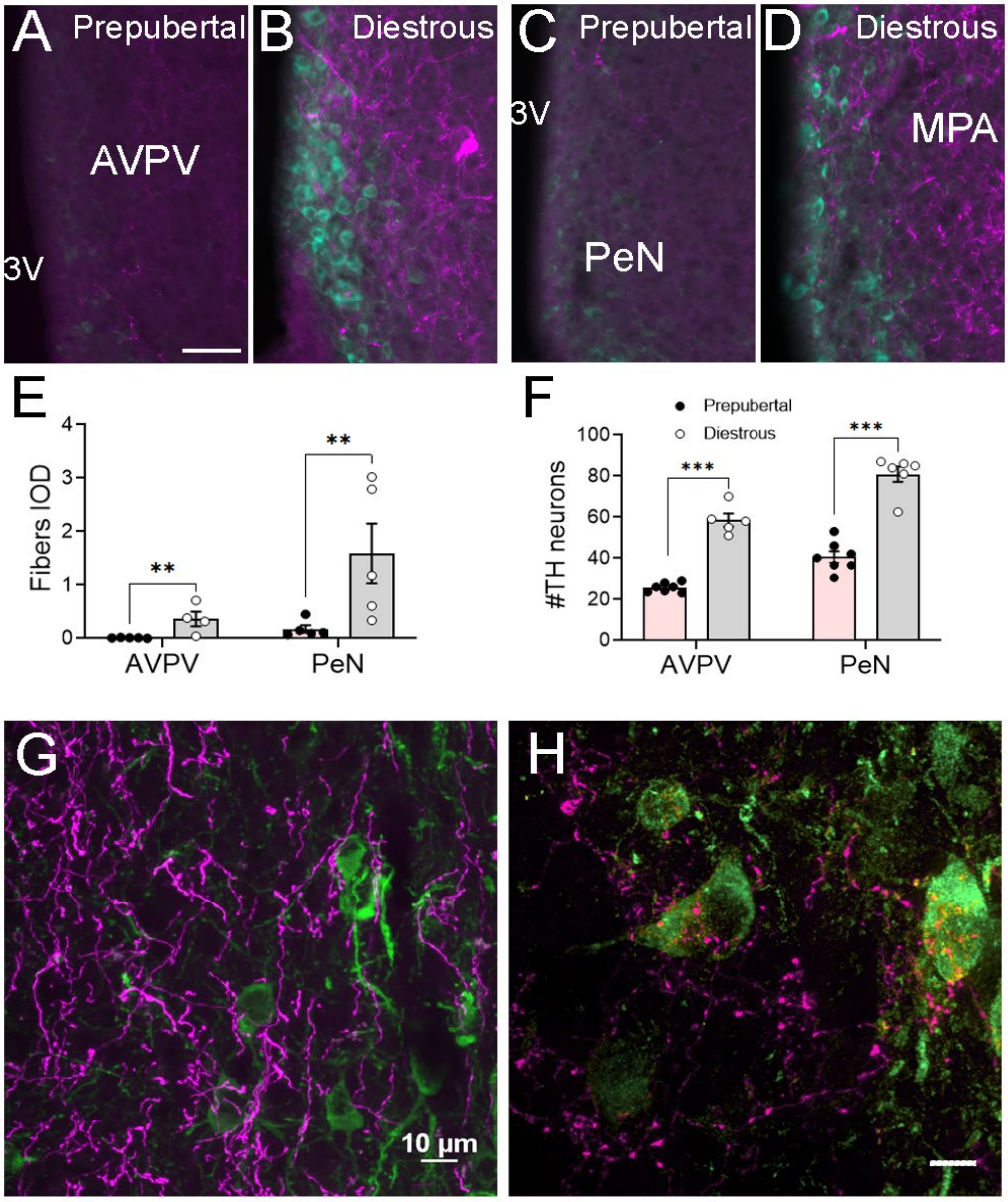


679

680 **Figure 7. DAT$^{Cre}$;tdTomato projections to dopaminergic cells in the anteroventral**
681 **periventricular and periventricular nuclei (AVPV/PeN) arise after puberty. A-D**.
682 Fluorescent images showing tdTomato (magenta) and tyrosine hydroxylase (TH)
683 immunoreactivity (green) in prepubertal (A, C) and in diestrous (B, D)
684 DAT$^{Cre}$;tdTomato females. **E.** Graph showing the quantification of the tdTomato fiber
685 density (Integrated optical density, IOD) in prepubertal *vs*. adult diestrous females in the
686 AVPV and the PeN areas. **F.** Graph showing the number of TH neurons per section in
687 the AVPV and in the PeN in prepubertal *vs*. diestrous female mice. **G.** Confocal
688 fluorescent maximum intensity projection image showing tdTomato (magenta) and TH

689 (green) cells and fibers in the lateral region of the AVPV/PeN in an adult diestrous
690 female. **H.** Higher magnification confocal fluorescent maximum intensity projection
691 image of a different field from G., showing tdTomato fibers in the PeN (magenta) and
692 the intense interaction of these projections to TH neurons (green) in this area. Scale bars
693 in A-D = 50 µm. G = 10 µm. H = 5 µm. ** $p<0.01$, *** $p<0.001$.

694 **References**


695 1. Cameron, J. L., Weltzin, T. E., McConaha, C., Helmreich, D. L., and Kaye, W.
696 H. (1991) Slowing of pulsatile luteinizing hormone secretion in men after forty-
697 eight hours of fasting. *J. Clin. Endocrinol. Metab.* **73**, 35–41

698 2. Kennedy, G. and Mitra, J. (1963) Body weight and food intake as initiating
699 factors for puberty in the rat. *J. Physiol.* **166**, 408–418

700 3. Cagampang, F., Maeda, K., Yokoyama, A., and Ota, K. (1990) Effect of food
701 deprivation on the pulsatile LH release in the cycling and ovariectomized female
702 rat. *Horm. Metab. Res.* **22**, 269–272

703 4. Donato, J., Silva, R. J., Sita, L. V, Lee, S., Lee, C., Lacchini, S., Bittencourt, J.
704 C., Franci, C. R., Canteras, N. S., and Elias, C. F. (2009) The ventral
705 premammillary nucleus links fasting-induced changes in leptin levels and
706 coordinated luteinizing hormone secretion. *J. Neurosci.* **29**, 5240–5250

707 5. Biro, F. M., Khoury, P., and Morrison, J. A. (2006) Influence of obesity on
708 timing of puberty. *Int. J. Androl.* **29**, 272–277

709 6. Burt Solorzano, C. M. and McCartney, C. R. (2010) Obesity and the pubertal
710 transition in girls and boys. *Reproduction* **140**, 399–410

711 7. Mahany, E. B., Han, X., Borges, B. C., Da Silveira Cruz-Machado, S., Allen, S.
712 J., Garcia-Galiano, D., Hoenerhoff, M. J., Bellefontaine, N. H., and Elias, C. F.
713 (2018) Obesity and High-Fat Diet Induce Distinct Changes in Placental Gene
714 Expression and Pregnancy Outcome. *Endocrinology* **159**, 1718–1733

715 8. Hill, J. W. and Elias, C. F. (2018) Neuroanatomical Framework of the Metabolic
716 Control of Reproduction. *Physiol. Rev.* **98**, 2349–2380

717 9. Anderson, G. M., Hill, J. W., Kaiser, U. B., Navarro, V. M., Ong, K. K., Perry, J.
718 R. B., Prevot, V., Tena-Sempere, M., and Elias, C. F. (2024) Metabolic control of
719 puberty: 60 years in the footsteps of Kennedy and Mitra's seminal work. *Nat.*
720 *Rev. Endocrinol.* **20**, 111–123

721 10. Quennell, J. H., Mulligan, A. C., Tups, A., Liu, X., Phipps, S. J., Kemp, C. J.,
722 Herbison, A. E., Grattan, D. R., and Anderson, G. M. (2009) Leptin indirectly
723 regulates gonadotropin-releasing hormone neuronal function. *Endocrinology* **150**,
724 2805–2812

725 11. Ahima, R. S., Prabakaran, D., Mantzoros, C., Qu, D., Lowell, B., Maratos-flier,
726 E., and Flier, J. S. (1996) Role of leptin in neuroendocrine response to fasting.
727 *Nature* **382**, 250–252

728 12. Ahima, R. S., Dushay, J., Flier, S. N., Prabakaran, D., and Flier, J. S. (1997)

729 Leptin accelerates the onset of puberty in normal female mice. *J. Clin. Invest.* **99**,
730 391–395

731 13. Farooqi, I. S., Wangensteen, T., Collins, S., Kimber, W., Matarese, G., Keogh, J.
732 M., Lank, E., Bottomley, B., Lopez-Fernandez, J., Ferraz-Amaro, I., Dattani, M.
733 T., Ercan, O., Myhre, A. G., Retterstol, L., Stanhope, R., Edge, J. A., Mckenzie,
734 S., Lessan, N., Ghodsi, M., De Rosa, V., Perna, F., Fontana, S., Barroso, I.,
735 Undlien, D. E., and O'Rahilly, S. (2007) Clinical and Molecular Genetic
736 Spectrum of Congenital Deficiency of the Leptin Receptor. *N. Engl. J. Med.* **356**,
737 237–247

738 14. De Luca, C., Kowalski, T. J., Zhang, Y., Elmquist, J. K., Lee, C., Kilimann, M.
739 W., Ludwig, T., Liu, S. M., and Chua, S. C. (2005) Complete rescue of obesity,
740 diabetes, and infertility in db/db mice by neuron-specific LEPR-B transgenes. *J.*
741 *Clin. Invest.* **115**, 3484–3493

742 15. Tartaglia, L. A., Dembski, M., Weng, X., Deng, N., Culpepper, J., Devos, R.,
743 Richards, G. J., Campfield, L. A., Clark, F. T., Deeds, J., Muir, C., Sanker, S.,
744 Moriarty, A., Moore, K. J., Smutko, J. S., Mays, G. G., Woolf, E. A., Monroe, C.
745 A., and Tepper, R. I. (1995) Identification and expression cloning of a leptin
746 receptor, OB-R. *Cell* **83**, 1263–71

747 16. Donato, J., Cravo, R. M., Frazão, R., Gautron, L., Scott, M. M., Lachey, J.,
748 Castro, I. A., Margatho, L. O., Lee, S., Lee, C., Richardson, J. A., Friedman, J.,
749 Chua, S., Coppari, R., Zigman, J. M., Elmquist, J. K., and Elias, C. F. (2011)
750 Leptin's effect on puberty in mice is relayed by the ventral premammillary
751 nucleus and does not require signaling in Kiss1 neurons. *J. Clin. Invest.* **121**,
752 355–368

753 17. Scott, M. M., Lachey, J. L., Sternson, S. M., Lee, C. E., Elias, C. F., Friedman, J.
754 M., and Elmquist, J. K. (2009) Leptin targets in the mouse brain. *J. Comp.*
755 *Neurol.* **514**, 518–532

756 18. Leshan, R. L., Louis, G. W., Jo, Y. H., Rhodes, C. J., Münzberg, H., and Myers,
757 M. G. (2009) Direct innervation of GnRH neurons by metabolic- and sexual
758 odorant-sensing leptin receptor neurons in the hypothalamic ventral
759 premammillary nucleus. *J. Neurosci.* **29**, 3138–3147

760 19. Louis, G. W., Greenwald-Yarnell, M., Phillips, R., Coolen, L. M., Lehman, M.
761 N., and Myers, M. G. (2011) Molecular mapping of the neural pathways linking
762 leptin to the neuroendocrine reproductive axis. *Endocrinology* **152**, 2302–2310

763 20. Sáenz de Miera, C., Bellefontaine, N., Allen, S. J., Myers, M. G., and Elias, C. F.
764 (2024) Glutamate neurotransmission from leptin receptor cells is required for
765 typical puberty and reproductive function in female mice. *Elife* **13**, RP93204

766 21. Ross, R. A., Leon, S., Madara, J. C., Schafer, D., Fergani, C., Maguire, C. A.,
767 Verstegen, A. M. J., Brengle, E., Kong, D., Herbison, A. E., Kaiser, U. B.,
768 Lowell, B. B., and Navarro, V. M. (2018) PACAP neurons in the ventral
769 premammillary nucleus regulate reproductive function in the female mouse. *Elife*
770 **7**, e35960

771 22. Williams, K. W., Sohn, J.-W., Donato, J., Lee, C. E., Zhao, J. J., Elmquist, J. K.,
772 and Elias, C. F. (2011) The acute effects of leptin require PI3K signaling in the

773 hypothalamic ventral premammillary nucleus. *J. Neurosci.* **31**, 13147–13156

774 23. Boehm, U., Zou, Z., and Buck, L. B. (2005) Feedback loops link odor and
775 pheromone signaling with reproduction. *Cell* **123**, 683–695

776 24. Meister, B. and Elde, R. (1993) Dopamine transporter mRNA in neurons of the
777 rat hypothalamus. *Neuroendocrinology* **58**, 388–395

778 25. Soden, M. E., Miller, S. M., Burgeno, L. M., Phillips, P. E. M., Hnasko, T. S.,
779 and Zweifel, L. S. (2016) Genetic Isolation of Hypothalamic Neurons that
780 Regulate Context-Specific Male Social Behavior. *Cell Rep.* **16**, 304–313

781 26. Stagkourakis, S., Spigolon, G., Williams, P., Protzmann, J., Fisone, G., and
782 Broberger, C. (2018) A neural network for intermale aggression to establish
783 social hierarchy. *Nat. Neurosci.* **21**, 834–842

784 27. Yip, S. H., York, J., Hyland, B., Bunn, S. J., and Grattan, D. R. (2018)
785 Incomplete concordance of dopamine transporter Cre (DATIREScre)-mediated
786 recombination and tyrosine hydroxylase immunoreactivity in the mouse
787 forebrain. *J. Chem. Neuroanat.* **90**, 40–48

788 28. Chen, A.-X., Yan, J.-J., Zhang, W., Wang, L., Yu, Z.-X., Ding, X.-J., Wang, D.-
789 Y., Zhang, M., Zhang, Y.-L., Song, N., Jiao, Z.-L., Xu, C., Zhu, S.-J., and Xu,
790 X.-H. (2020) Specific Hypothalamic Neurons Required for Sensing Conspecific
791 Male Cues Relevant to Inter-male Aggression. *Neuron* **108**, 763-774.e6

792 29. Stagkourakis, S., Williams, P., Spigolon, G., Khanal, S., Ziegler, K., Heikkinen,
793 L., Fisone, G., and Broberger, C. (2024) Maternal Aggression Driven by the
794 Transient Mobilisation of a Dormant Hormone-Sensitive Circuit. *bioRxiv,* doi:
795 10.1101/2023.02.02.526862

796 30. Bäckman, C. M., Malik, N., Zhang, Y. J., Shan, L., Grinberg, A., Hoffer, B. J.,
797 Westphal, H., and Tomac, A. C. (2006) Characterization of a mouse strain
798 expressing Cre recombinase from the 3′ untranslated region of the dopamine
799 transporter locus. *Genesis* **44**, 383–390

800 31. Ekstrand, M. I., Terzioglu, M., Galter, D., Zhu, S., Hofstetter, C., Lindqvist, E.,
801 Thams, S., Bergstrand, A., Hansson, F. S., Trifunovic, A., Hoffer, B., Cullheim,
802 S., Mohammed, A. H., Olson, L., and Larsson, N. G. (2007) Progressive
803 parkinsonism in mice with respiratory-chain-deficient dopamine neurons. *Proc.*
804 *Natl. Acad. Sci. U. S. A.* **104**, 1325–1330

805 32. Cravo, R. M., Frazao, R., Perello, M., Osborne-Lawrence, S., Williams, K. W.,
806 Zigman, J. M., Vianna, C., and Elias, C. F. (2013) Leptin Signaling in Kiss1
807 Neurons Arises after Pubertal Development. *PLoS One* **8**, e58698

808 33. Donato, J. J., Lee, C., Ratra, D., Franci, C., Canteras, N., and Elias, C. (2013)
809 Lesions of the ventral premammillary nucleus disrupt the dynamic changes in
810 kiss1 and gnrh expression characteristic of the proestrus – estrus transition.
811 *Neuroscience* **241**, 67–79

812 34. Krashes, M. J., Roth, B. L., Lowell, B. B., Koda, S., Ye, C., Rogan, S. C.,
813 Adams, A. C., Cusher, D. S., and Maratos-flier, E. (2011) Rapid, reversible
814 activation of AgRP neurons drives feeding behavior in mice. *J. Clin. Invest.* **121**,
815 1424–1428

35. Sáenz de Miera, C., Feng, J., Elias, C. F., and Qi, N. (2023) Remote Neuronal Activation Coupled with Automated Blood Sampling to Induce and Measure Circulating Luteinizing Hormone in Mice. *J. Vis. Exp.* **198**, e65875

36. Han, X., Burger, L. L., Garcia-Galiano, D., Sim, S., Allen, S. J., Olson, D. P., Myers, M. G., and Elias, C. F. (2020) Hypothalamic and Cell-Specific Transcriptomes Unravel a Dynamic Neuropil Remodeling in Leptin-Induced and Typical Pubertal Transition in Female Mice. *iScience* **23**, 101563

37. Ingalls, A. M., Dickie, M. M., and Snell, G. D. (1950) Obese, a new mutation in the house mouse. *J. Hered.* **41**, 315–317

38. Bohlen, T. M., Silveira, M. A., Zampieri, T. T., Frazão, R., and Donato, J. (2016) Fatness rather than leptin sensitivity determines the timing of puberty in female mice. *Mol. Cell. Endocrinol.* **423**, 11–21

39. Castellano, J. M., Bentsen, A. H., Sánchez-Garrido, M. A., Ruiz-Pino, F., Romero, M., Garcia-Galiano, D., Aguilar, E., Pinilla, L., Diéguez, C., Mikkelsen, J. D., and Tena-Sempere, M. (2011) Early metabolic programming of puberty onset: Impact of changes in postnatal feeding and rearing conditions on the timing of puberty and development of the hypothalamic kisspeptin system. *Endocrinology* **152**, 3396–3408

40. Semaan, S. J., Murray, E. K., Poling, M. C., Dhamija, S., Forger, N. G., and Kauffman, A. S. (2010) BAX-dependent and BAX-independent regulation of Kiss1 neuron development in mice. *Endocrinology* **151**, 5807–5817

41. Clarkson, J. and Herbison, A. E. (2011) Dual Phenotype Kisspeptin-Dopamine Neurones of the Rostral Periventricular Area. *J. Neuroendocrinol.* **23**, 293–301

42. Kumar, D., Candlish, M., Periasamy, V., Avcu, N., Mayer, C., and Boehm, U. (2015) Specialized subpopulations of kisspeptin neurons communicate with gnrh neurons in female mice. *Endocrinology* **156**, 32–38

43. Stephens, S. B., Rouse, M. L., Tolson, K. P., Liaw, R. B., Parra, R. A., Chahal, N., and Kauffman, A. S. (2017) Effects of selective deletion of tyrosine hydroxylase from kisspeptin cells on puberty and reproduction in male and female mice. *eNeuro* **4**, e0150-17.2017

44. Clarkson, J., Boon, W. C., Simpson, E. R., and Herbison, A. E. (2009) Postnatal development of an estradiol-kisspeptin positive feedback mechanism implicated in puberty onset. *Endocrinology* **150**, 3214–3220

45. Silveira, M. A., Zampieri, T. T., Furigo, I. C., Abdulkader, F., Donato, J., and Frazão, R. (2019) Acute effects of somatomammotropin hormones on neuronal components of the hypothalamic-pituitary-gonadal axis. *Brain Res.* **1714**, 210–217

46. Hoffman, B. J., Hansson, S. R., Mezey, É., and Palkovits, M. (1998) Localization and dynamic regulation of biogenic amine transporters in the mammalian central nervous system. *Front. Neuroendocrinol.* **19**, 187–231

47. Karasawa, N., Arai, R., Isomura, G., Yamada, K., Sakai, K., Sakai, M., Nagatsu, T., and Nagatsu, I. (1994) Phenotypic changes of AADC-only immunopositive premammillary neurons in the brain of laboratory shrew Suncus murinus by

859 systemic administration of monoamine precursors. *Neurosci. Lett.* **179**, 65–70

860 48. de Vriend, V. A., van ’t Sant, L. J., Rozeboom, A., Luijendijk-berg, M. C.,
861 Omrani, A., and Adan, R. A. (2021) Leptin Receptor Expressing Neurons in the
862 Substantia Nigra Regulate Locomotion , and in The Ventral Tegmental Area
863 Motivation and Feeding. *Front. Endocrinol.* **12**, 680494

864 49. Opland, D. M., Leinninger, G. M., and Myers, M. G. (2010) Modulation of the
865 mesolimbic dopamine system by leptin. *Brain Res.* **1350**, 65–70

866 50. Xu, Y., Lu, Y., Xu, P., Mangieri, L. R., Isingrini, E., Xu, Y., Giros, B., and Tong,
867 Q. (2017) VMAT2-mediated neurotransmission from midbrain leptin receptor
868 neurons in feeding regulation. *eNeuro* **4**, e0083-17.2017

869 51. Fulton, S., Pissios, P., Manchon, R. P., Stiles, L., Frank, L., Pothos, E. N.,
870 Maratos-Flier, E., and Flier, J. S. (2006) Leptin Regulation of the
871 Mesoaccumbens Dopamine Pathway. *Neuron* **51**, 811–822

872 52. Perry, M. L., Leinninger, G. M., Chen, R., Luderman, K. D., Yang, H., Gnegy,
873 M. E., Myers, M. G., and Kennedy, R. T. (2010) Leptin promotes dopamine
874 transporter and tyrosine hydroxylase activity in the nucleus accumbens of
875 Sprague-Dawley rats. *J. Neurochem.* **114**, 666–674

876 53. Amara, S. G. and Kuhar, M. J. (1993) Neurotransmitter Transporters: Recent
877 progress. *Annu. Rev. Neurosci.* **16**, 73–93

878 54. Merlino, D. J., Barton, J. R., Charsar, B. A., Byrne, M. D., Rappaport, J. A.,
879 Smeyne, R. J., Lepore, A. C., Snook, A. E., and Waldman, S. A. (2019) Two
880 distinct GUCY2C circuits with PMV (hypothalamic) and SN/VTA (midbrain)
881 origin. *Brain Struct. Funct.* **224**, 2983–2999

882 55. Wang, L., Vanacker, C., Burger, L. L., Barnes, T., Shah, Y. M., Myers, M. G.,
883 and Moenter, S. M. (2019) Genetic dissection of the different roles of
884 hypothalamic kisspeptin neurons in regulating female reproduction. *Elife* **8**,
885 e43999

886 56. Wagenmaker, E. R. and Moenter, S. M. (2017) Exposure to acute psychosocial
887 stress disrupts the luteinizing hormone surge independent of estrous cycle
888 alterations in female mice. *Endocrinology* **158**, 2593–2602

889 57. Beltramino, C. and Taleisnik, S. (1985) Ventral premammillary nuclei mediate
890 pheromonal-induced LH release stimuli in the rat. *Neuroendocrinology* **41**, 119–
891 124

892 58. Bleier, R., Byne, W., and Siggelkow, I. (1982) Cytoarchitectonic sexual
893 dimorphisms of the medial preoptic and anterior hypothalamic areas in guinea
894 pig, rat, hamster, and mouse. *J. Comp. Neurol.* **212**, 118–130

895 59. Simerly, R. B., Swanson, L. W., and Gorski, R. A. (1985) The distribution of
896 monoaminergic cells and fibers in a periventricular preoptic nucleus involved in
897 the control of gonadotropin release: Immunohistochemical evidence for a
898 dopaminergic sexual dimorphism. *Brain Res.* **330**, 55–64

899 60. Simerly, R. B., Zee, M. C., Pendleton, J. W., Lubahn, D. B., and Korach, K. S.
900 (1997) Estrogen receptor-dependent sexual differentiation of dopaminergic
901 neurons in the preoptic region of the mouse. *Proc. Natl. Acad. Sci. U. S. A.* **94**,

902 14077–14082

903 61. Clarkson, J. and Herbison, A. E. (2006) Postnatal development of kisspeptin
904 neurons in mouse hypothalamus; sexual dimorphism and projections to
905 gonadotropin-releasing hormone neurons. *Endocrinology* **147**, 5817–5825

906 62. Björklund, A. and Hökfelt, T., eds. (1984) Handbook of Chemical
907 Neuroanatomy. Vol 2: Classical Transmitters in the CNS. Part 1. Elsevier
908 Science Publishers B.V.

909 63. Lorang, D., Amara, S. G., and Simerly, R. B. (1994) Cell-type-specific
910 expression of catecholamine transporters in the rat brain. *J. Neurosci.* **14**, 4903–
911 4914

912 64. Ciliax, B. J., Drash, G. W., Staley, J. K., Haber, S., Mobley, C. J., Miller, G. W.,
913 Mufson, E. J., Mash, D. C., and Levey, A. I. (1999) Immunocytochemical
914 localization of the dopamine transporter in human brain. *J. Comp. Neurol.* **409**,
915 38–56

916 65. Stagkourakis, S., Kim, H., Lyons, D. J., and Broberger, C. (2016) Dopamine
917 Autoreceptor Regulation of a Hypothalamic Dopaminergic Network. *Cell Rep.*
918 **15**, 735–747

919 66. Scott, N., Prigge, M., Yizhar, O., and Kimchi, T. (2015) A sexually dimorphic
920 hypothalamic circuit controls maternal care and oxytocin secretion. *Nature* **525**,
921 519–522

922

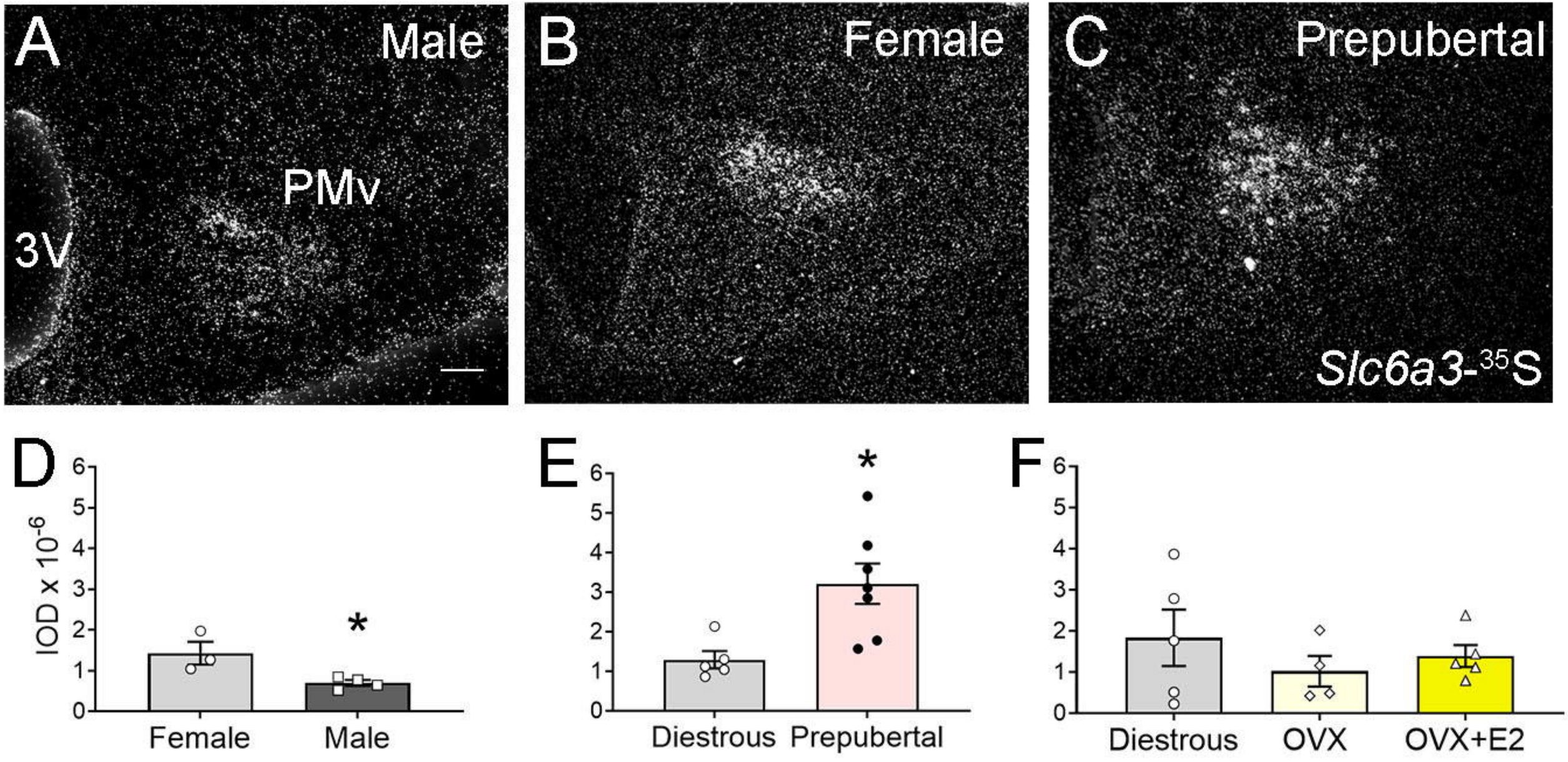
A
Male
PMv
3V
B
Female
C
Prepubertal
Slc6a3-35S
D
IOD x 10-6
6
5
4
3
2
1
0
*
Female
Male
E
6
5
4
3
2
1
0
*
Diestrous
Prepubertal
F
6
5
4
3
2
1
0
Diestrous
OVX
OVX+E2

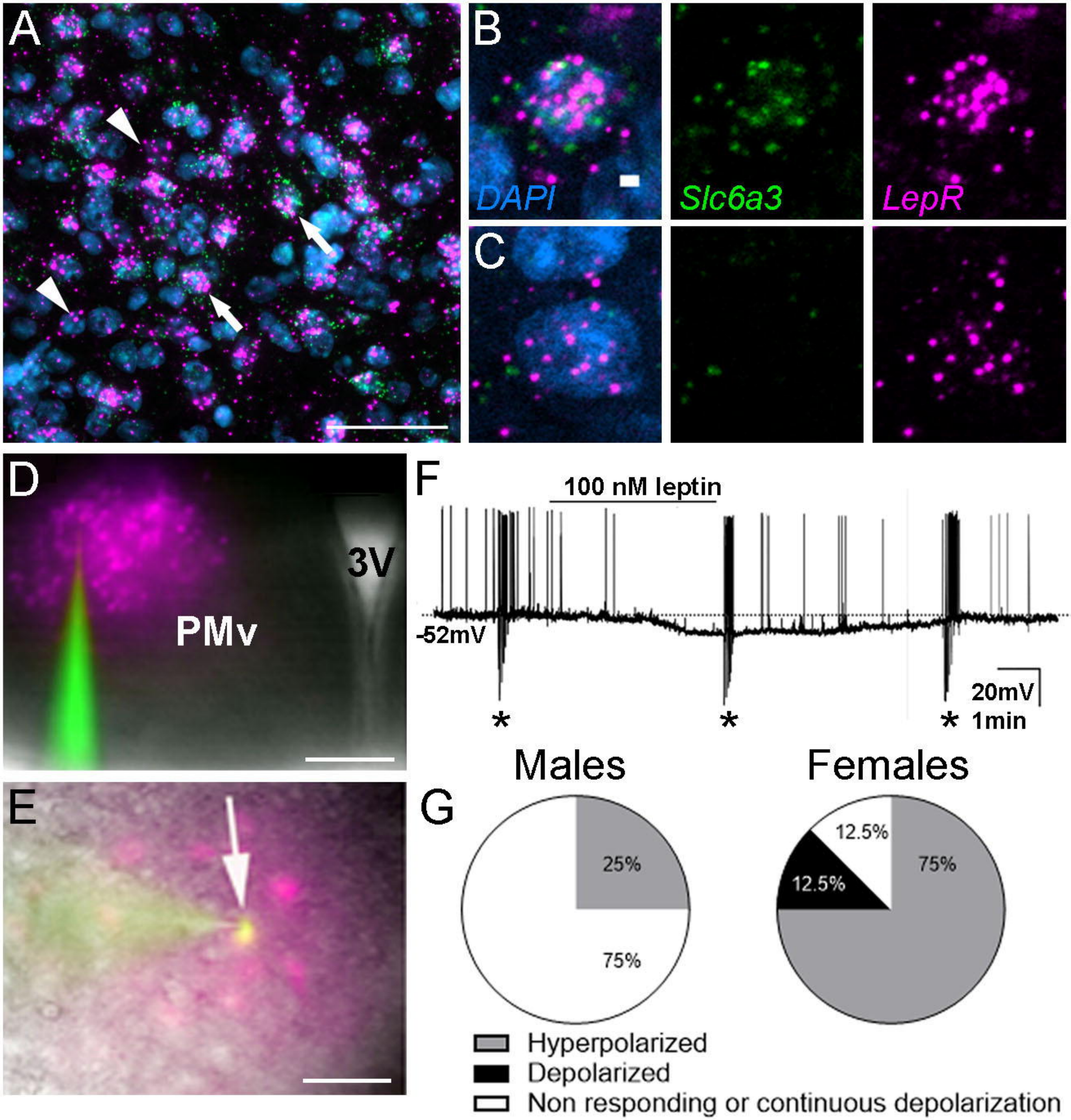
A
B
DAPI
Slc6a3
LepR
C
D
3V
PMv
E
F
100 nM leptin
-52mV
20mV
1min
Males
Females
G
25%
75%
12.5%
12.5%
75%
Hyperpolarized
Depolarized
Non responding or continuous depolarization

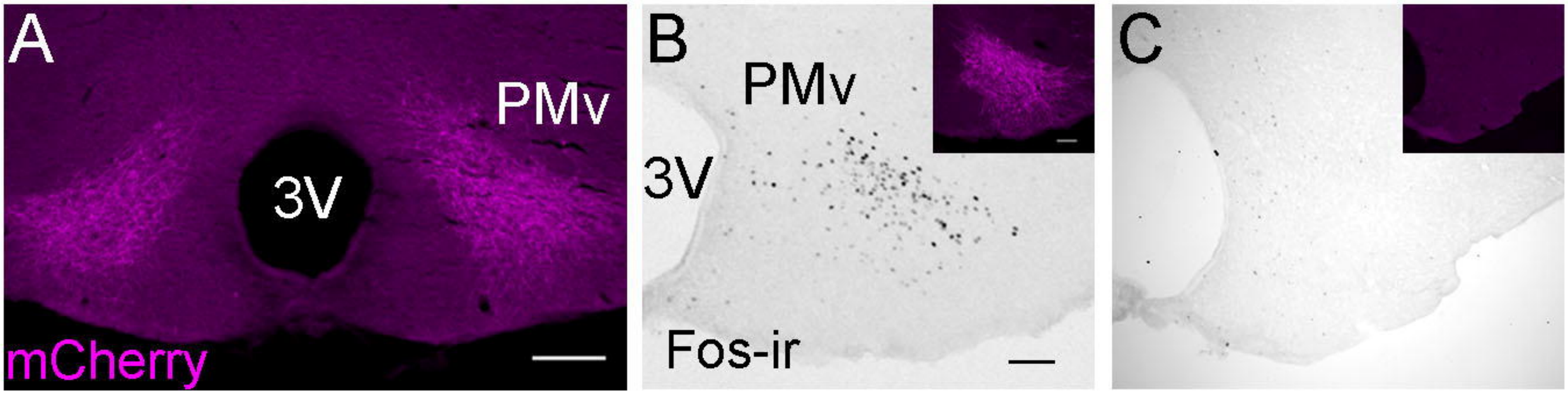
A
PMv
3V
mCherry
B
PMv
3V
Fos-ir
C

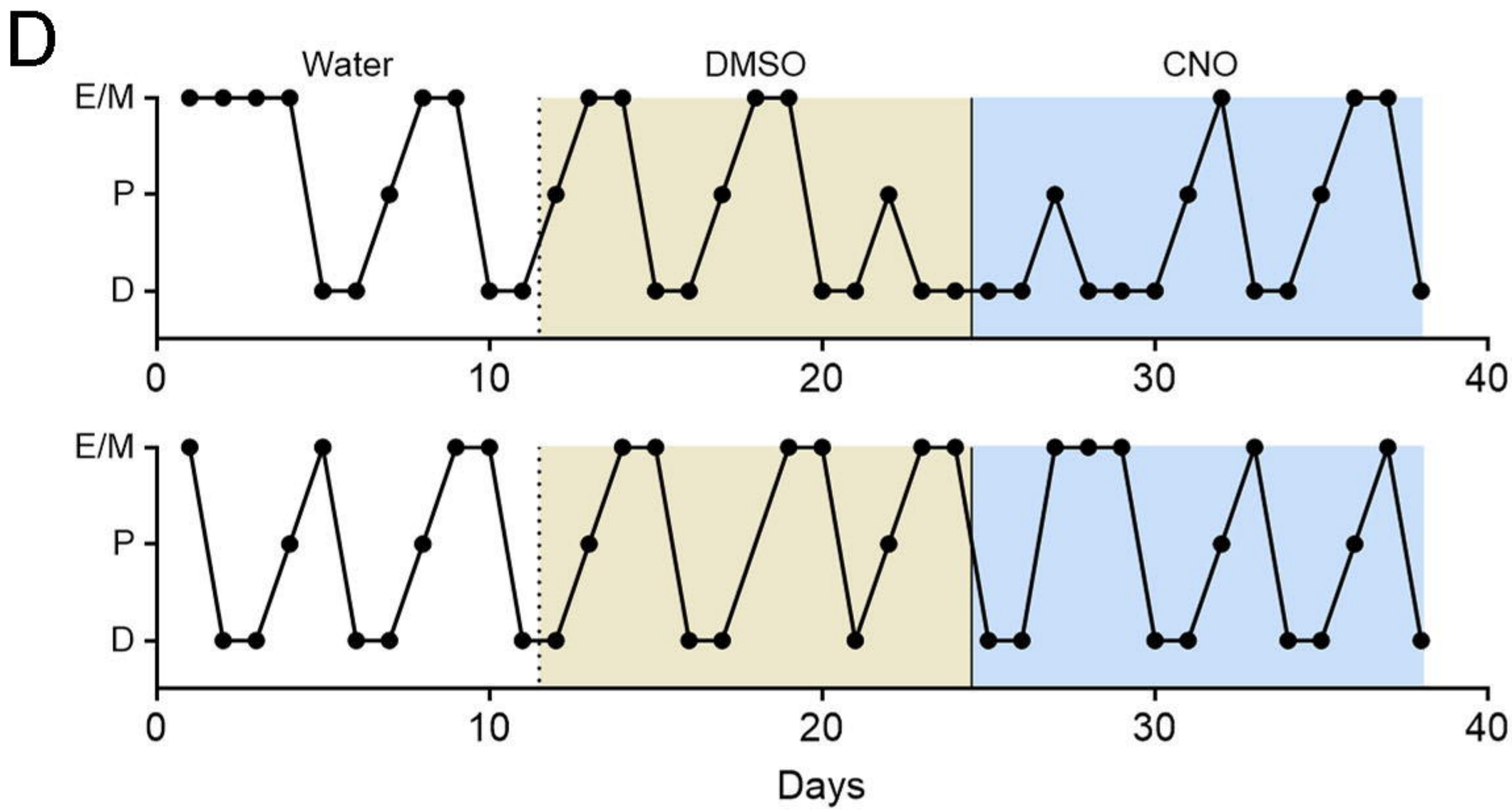
D
Water
DMSO
CNO
E/M
P
D
0
10
20
30
40
Days

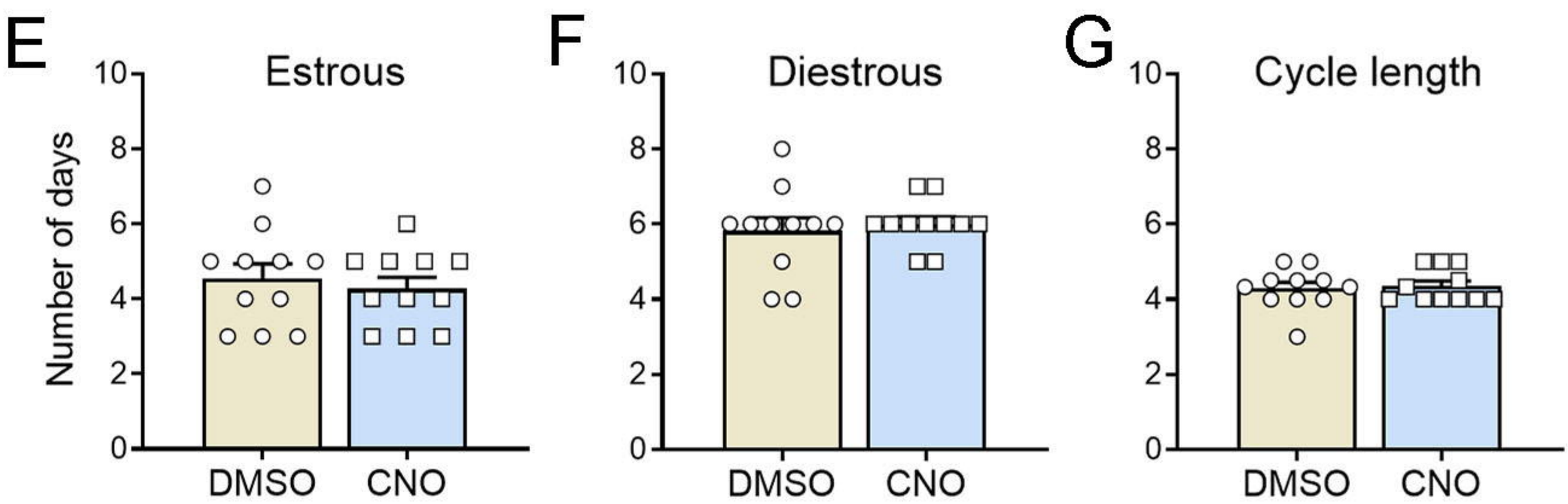
E
Estrous
F
Diestrous
G
Cycle length
Number of days
0
2
4
6
8
10
DMSO
CNO

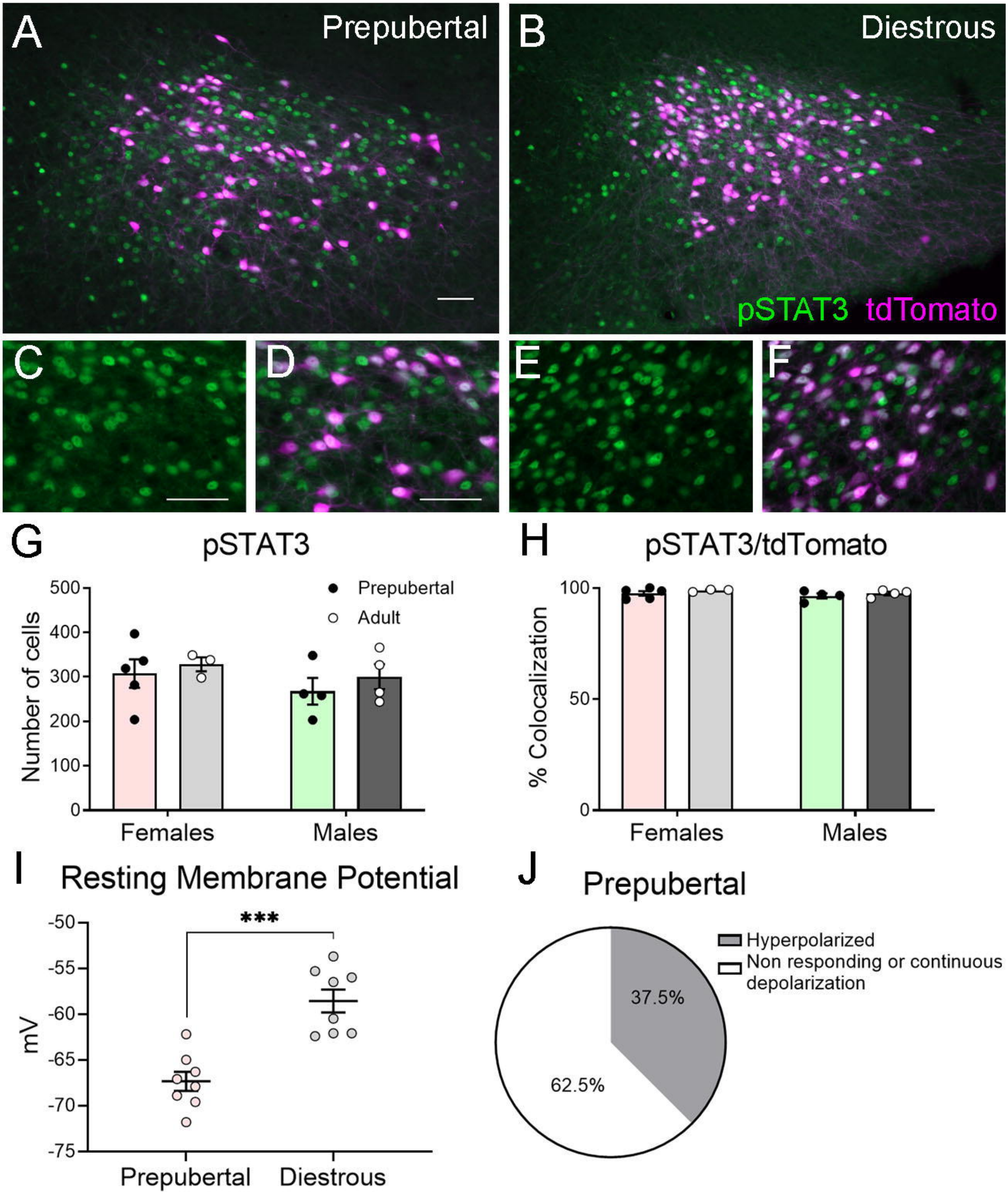
A
Prepubertal
B
Diestrous
pSTAT3 tdTomato
C
D
E
F
G
pSTAT3
Prepubertal
Adult
Number of cells
500
400
300
200
100
0
Females
Males
H
pSTAT3/tdTomato
% Colocalization
100
50
0
Females
Males
I
Resting Membrane Potential
***
mV
-50
-55
-60
-65
-70
-75
Prepubertal
Diestrous
J
Prepubertal
Hyperpolarized
Non responding or continuous depolarization
37.5%
62.5%

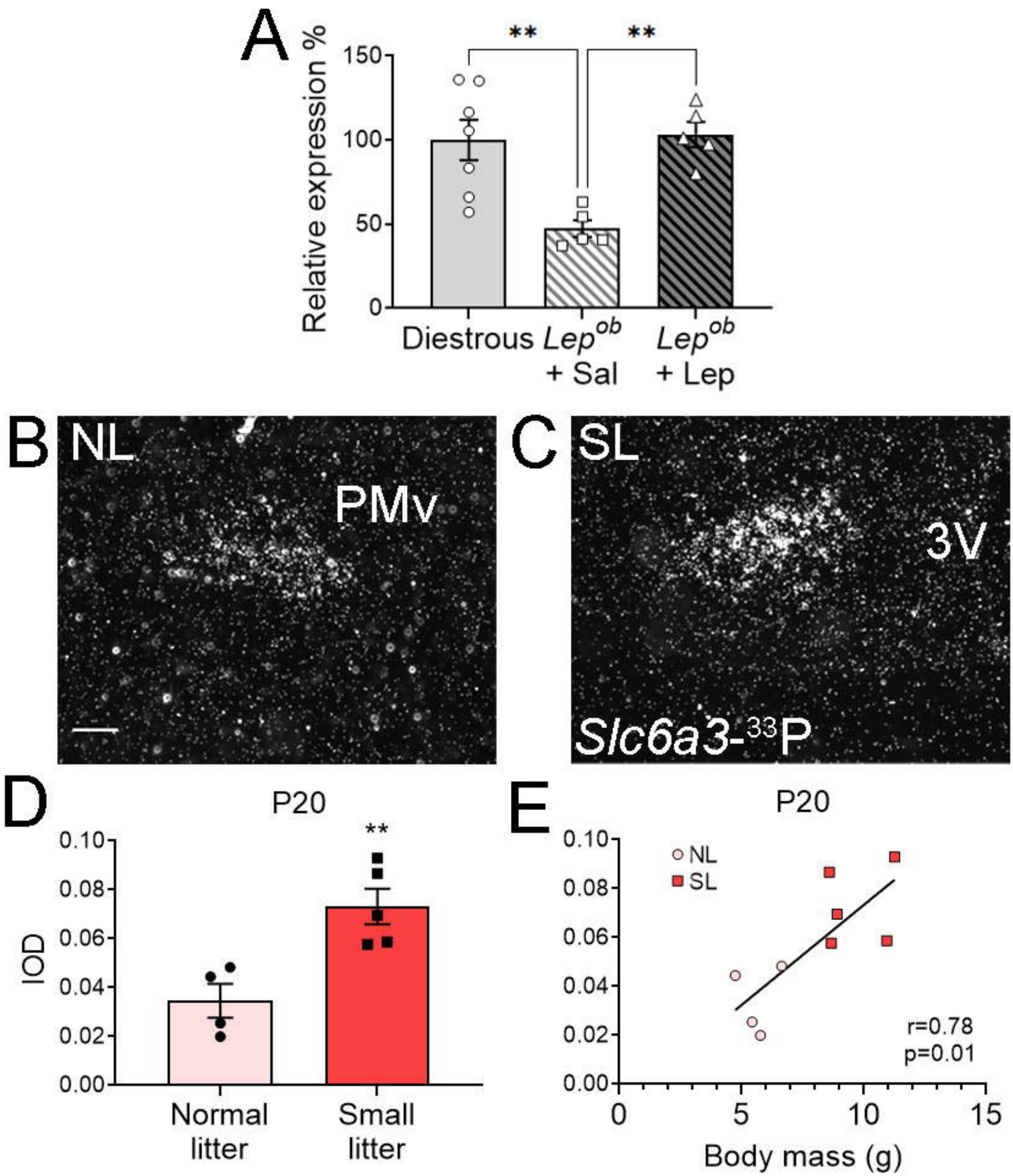
A
Relative expression %
150
100
50
0
**
**
Diestrous
Lep^ob + Sal
Lep^ob + Lep
B
NL
PMv
C
SL
3V
Slc6a3-33P
D
P20
IOD
0.10
0.08
0.06
0.04
0.02
0.00
**
Normal litter
Small litter
E
P20
NL
SL
r=0.78
p=0.01
0
5
10
15
Body mass (g)

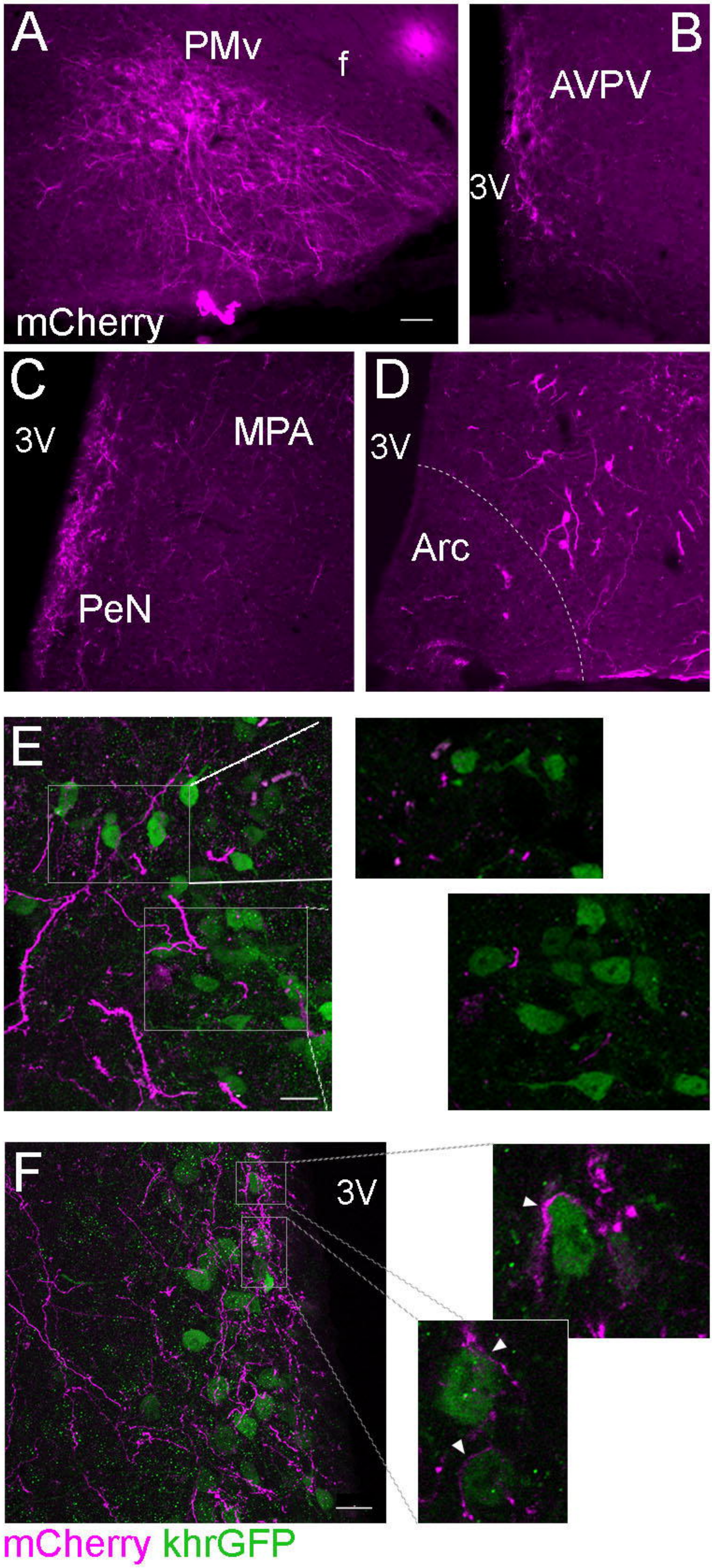
A
PMv
f
mCherry
B
AVPV
3V
C
3V
MPA
PeN
D
3V
Arc
E
F
3V
mCherry khrGFP

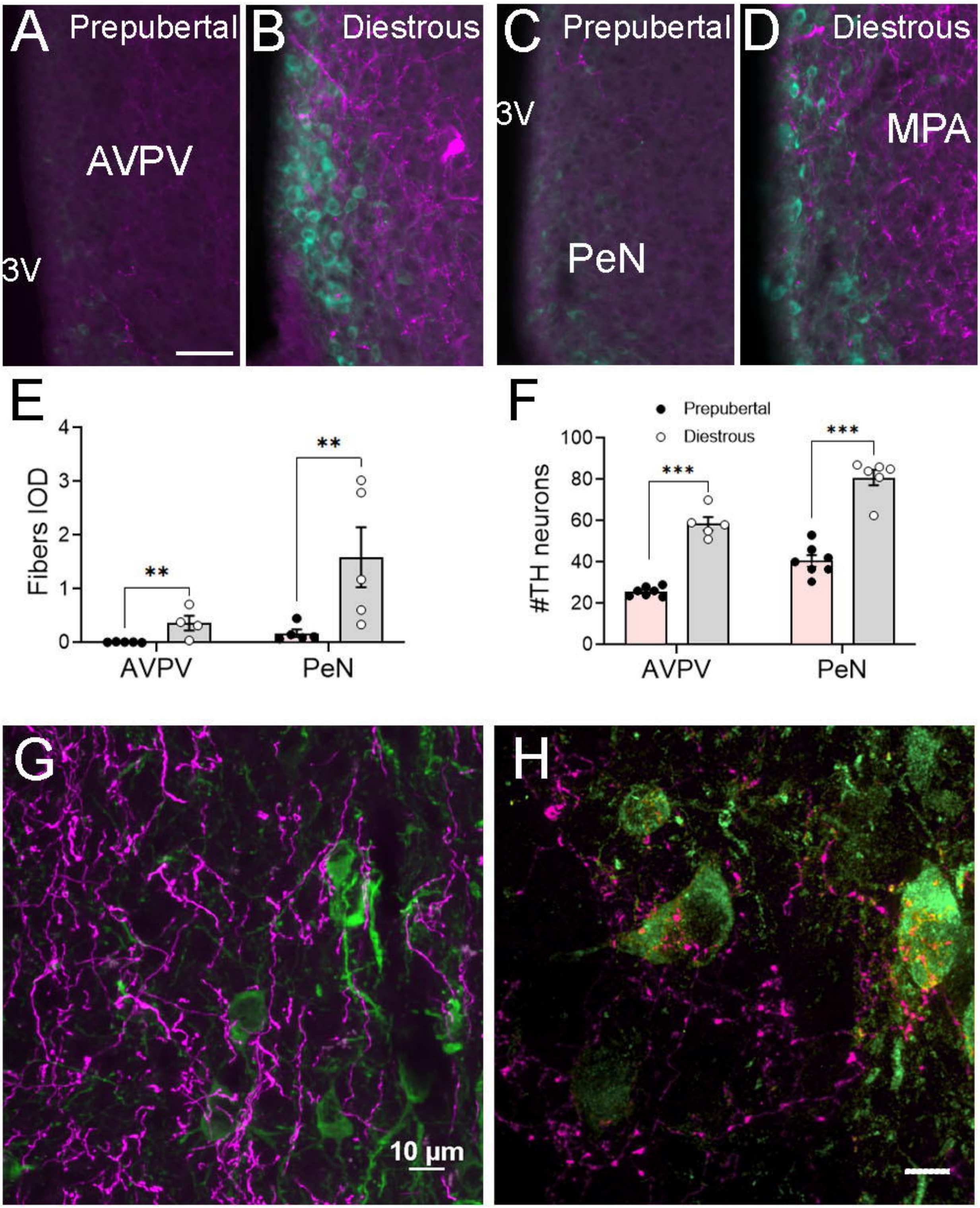
A
Prepubertal
AVPV
3V
B
Diestrous
C
Prepubertal
3V
PeN
D
Diestrous
MPA
E
Fibers IOD
4
3
2
1
0
**
**
AVPV
PeN
F
Prepubertal
Diestrous
#TH neurons
100
80
60
40
20
0
***
***
AVPV
PeN
G
10 µm
H